INSTITUTO TECNOLÓGICO
Y DE ESTUDIOS SUPERIORES DE OCCIDENTE

Reconocimiento de validez oficial de estudios de nivel superior según acuerdo secretarial 15018, publicado en el Diario Oficial de la Federación el 29 de noviembre de 1976.

Departamento de Electrónica, Sistemas e Informática

DOCTORADO EN CIENCIAS DE LA INGENIERÍA

DISEÑO ÓPTIMO DE SENSORES NANOESTRUCTURADOS: UN ENFOQUE BASADO EN LA METODOLOGÍA DE SUPERFICIE DE RESPUESTA

Tesis que para obtener el grado de

DOCTOR EN CIENCIAS DE LA INGENIERÍA

presenta: Patricia Guadalupe López Cárdenas

Director de tesis: Dr. Elsie Evelyn Araujo Palomo

Co-director de tesis: Dr. Juan Diego Sánchez Torres

Tlaquepaque, Jalisco. Septiembre de 2023

DOCTOR EN CIENCIAS DE LA INGENIERÍA (2022) ITESO, Tlaquepaque, Jal., México

TÍTULO: **Diseño óptimo de sensores nanoestructurados: un enfoque basado en la metodología de superficie de respuesta**

AUTOR: Patricia Guadalupe López Cárdenas
Químico Farmacéutico Biólogo (UAG, México)
Maestro en Ingeniería para la Calidad (ITESO, México)

DIRECTOR DE TESIS: Elsie Evelyn Araujo Palomo
Departamento de Matemáticas y Física, ITESO
Licenciado en Matemáticas (UASLP, México)
Maestro en Metalurgia e Ingeniería de Materiales (UASLP, México)
Doctor en Ingeniería y Ciencias de Materiales (UASLP, México)

NUMBER OF PAGES: xxiii, 89

ITESO – The Jesuit University of Guadalajara

Department of Electronics, Systems, and Informatics

DOCTORAL PROGRAM IN ENGINEERING SCIENCES

OPTIMAL DESIGN OF NANOSTRUCTURED SENSORS: AN APPROACH BASED ON THE RESPONSE SURFACE METHODOLOGY

Thesis to obtain the degree of

DOCTOR IN ENGINEERING SCIENCES

Presents: Patricia Guadalupe López Cárdenas

Thesis Director: Dr. Elsie Evelyn Araujo Palomo

Thesis Co-director: Dr. Juan Diego Sánchez Torres

Tlaquepaque, Jalisco, Mexico
September 2023

PHD IN ENGINEERING SCIENCES (2022) ITESO, Tlaquepaque, Jal., Mexico

TITLE: **Optimal Design of Nanostructured Sensors: an Approach Based on the Response Surface Methodology**

AUTHOR: Patricia Guadalupe López Cárdenas
Bachelor's degree in biological pharmaceutical chemistry (UAG, Mexico)
Master's degree in quality engineering (ITESO, Mexico)

THESIS DIRECTOR: Elsie Evelyn Araujo Palomo
Department of Mathematics and Physics, ITESO
Bachelor's degree in mathematics (UASLP, México)
Master's degree in metallurgy and material engineering (UASLP, México)
Ph.D. degree in materials sciences and engineering (UASLP, Mexico)

NUMBER OF PAGES: xxiii, **89**

I dedicate this enormous effort and work with special affection to my husband, Eng. Eduardo Medina Barron, and to my sons, LT. Eduardo Medina Lopez and AR. Alvaro Medina Lopez and my dear granddaughter Ana Fernanda Medina Gutierrez for their patience, love, motivation, incentive, support, and continuous reinforcement to achieve my goal.

I also want to thank my dear sisters, brothers, and relatives, for their constant encouragement to continue studying. To my friends for incentivizing me to continue my studies. To God for keeping me strong with my faith and his strength.

Resumen

En los últimos años se han desarrollado sensores de muchos tipos y para una gran variedad de usos o aplicaciones. En esta tesis, se presenta un enfoque basado en datos para optimizar el diseño de sensores altamente sensible al peróxido de hidrógeno (H_2O_2) basados en arreglos de nanoalambres auto soportados de níquel (Ni NW), utilizando la metodología de superficie de respuesta (RSM). Los nanoalambres (NW) fueron desarrollados por la técnica de síntesis electroquímica asistida por membranas nanoporosas que fungen como moldes, utilizando como metal los iones de níquel para el crecimiento de los nanoalambres. RSM es aplicada utilizando datos experimentales obtenidos por voltamperometría cíclica (CV) optimizando el diseño de estos sensores nanoestructurados para detectar H_2O_2. El objetivo es mejorar el rendimiento del sensor variando la longitud de Ni NW al modificar las condiciones de trabajo, incluyendo la concentración de H_2O_2 y el potencial de medición aplicado. Se empleó con éxito RSM logrando identificar las condiciones teóricas óptimas para el sensor: con una longitud de NW de 2.64 μm, una concentración de 3.25 mM H_2O_2 y un potencial de detección de 0.02 V. Se fabricó un sensor con la longitud óptima de los nanoalambres obtenida por el modelo y se validó su rendimiento, comparándolo con sensores de diferentes longitudes de nanoalambres: un sensor plano de Ni; y otro sensor nanoestructurado Ni NW. El sensor optimizado logra una reducción del 50 % en el límite de detección (LOD) al H_2O_2 y un aumento del 18 % en sensibilidad al H_2O_2, respecto al sensor nanoestructurado. El sensor optimizado es al menos 35 veces más sensible para detectar H_2O_2 que sensores con geometrías planas, de uso estándar en aplicaciones comerciales. Estos resultados resaltan el potencial de RSM como una poderosa y rentable herramienta estadística para optimizar sensores nanoestructurados y acelerar el ciclo de diseño-construcción-prueba. El sensor de H_2O_2 optimizado se puede aplicar en la industria alimentaria, diagnóstico médico y monitoreo ambiental. Este sensor puede mejorar significativamente la detección de glucosa en muestras no invasivas como lágrimas y saliva al combinarlo con enzimas de glucosa oxidasa inmovilizadas, crucial en el continuo monitoreo de glucosa en pacientes con diabetes mellitus. RSM permite futuras extensiones para investigar otras variables de diseño y materiales de detección, así como optimizar los sensores para detectar diferentes sustancias, fomentando los avances en las tecnologías de sensores.

Summary

In recent years, numerous types of sensors have been developed for a wide variety of uses or applications. In this thesis, a data-driven approach is presented to optimize the design of highly sensitive hydrogen peroxide (H_2O_2) sensors based on self-supported nickel nanowire (Ni NW) arrays using response surface methodology (RSM). The nanowires (NW) were developed through the technique of electrochemical synthesis assisted with nanoporous membranes as templates, and nickel ions were used as metal for the growing of the nanowires. RSM is applied using experimental data obtained through cyclic voltammetry (CV) optimizing of the design of these nanostructured sensors to detect H_2O_2. The goal is to enhance the performance of the sensor through customizing the Ni NW length while optimizing the working conditions, including the H_2O_2 concentration and applied potential. RSM was successfully employed to identify the theoretical optimal conditions for the sensor: with a NW length of 2.64 μm, a concentration of 3.25 mM H_2O_2, and a detection potential of 0.02 V. A sensor with the optimal NW length was fabricated and validated its performance by comparison to sensors with different NW lengths, such as a planar Ni sensor, and against another nanostructured sensor Ni NW. The optimized sensor achieves a 50% reduction in limit of detection (LOD) to H_2O_2 and an 18% increase in sensitivity to H_2O_2, compared to the Ni NW sensor. Moreover, the optimized sensor is at least 35 times more sensitive for H_2O_2 detection than sensors with planar geometries, which are standard in commercial applications. The results highlight the potential of RSM as a powerful, cost-effective, and statistical tool for optimizing nanostructured sensors and accelerating the design-build-test cycle. Accurate detection of H_2O_2 enables effective monitoring, control, and optimization, leading to improved safety, quality assurance, environmental protection, and overall efficiency in these sectors. The optimized H_2O_2 nanostructured sensor can be applied in various fields, including medical diagnostics and environmental monitoring. This sensor can significantly enhance glucose detection in non-invasive samples such as tears and saliva when combined with immobilized glucose oxidase enzymes, which is crucial for continuous glucose monitoring in diabetes mellitus patients. The methodology presented in this thesis allows further extensions to investigate other design variables and sensing materials, as well as to optimize sensors for detecting different substances, fostering advancements in sensor technologies.

Acknowledgements

The author wishes to express her sincere appreciation to Dr. Elsie Evelyn Araujo Palomo, professor of the Department of Mathematics, and Physics at ITESO, for his encouragement, expert guidance, and keen supervision as doctoral thesis director throughout the course of this work. The author offers her gratitude to Dr. Juan Diego Sánchez-Torres, from professor of the Department of Mathematics, and Physics at ITESO, for his support as doctoral thesis co-director during the development of this work. She also thanks Dr. Mildred Quintana Ruiz, Dr. José Ernesto Rayas-Sánchez, and Dr. Edgar Briones Hernandez, members of this Ph.D. Thesis Committee, for their interest, assessment, and suggestions.

Special thanks are due to Dr. Jaime Emmanuel Alcalá Temores, from U de G and ITESO, for fruitful cooperation and helpful technical discussions.

It is the author's pleasure to acknowledge fruitful collaboration and stimulating discussions Dr. Riemann Ruiz Cruz, with her colleagues of Eleazar Benitez Nuñez for laboratory support, Dr. Yenny Velázquez Galván, and Guillermo González Arreola for SEM support, and Dr. Edgar Briones Hernández for the facilities in the metalized membrane.

The author gratefully acknowledges the financial assistance through a scholarship 751908 granted by the *Consejo Nacional de Ciencia y Tecnología* (CONACYT), Mexican Government, and for a partial scholarship of the financial support provided by *Programa de Superación del Nivel Académico* (PSNA ITESO).

Finally, special thanks are due to my family: to my husband Eng. Eduardo Medina Barron, also, to my sons LT. Eduardo Medina Lopez and AR. Alvaro Medina Lopez, in addition to my dear granddaughter, Ana Fernanda Medina Gutierrez, for their understanding, patience, and continuous loving support.

Contenido

Contents

List of Figures

List of Tables

Introduction

Nanostructured sensors have quickly become a cutting-edge and cost-effective technology for detecting low concentrations of substances in samples, particularly for clinical applications, industrial processes, and environmental monitoring [López-Cárdenas-21b], [López-Cárdenas-23b], [Wang-17], [Ghanei-Motlagh-19], and [Zhang-23].

Nanostructured sensors offer enhanced qualities of sensitivity, selectivity, and miniaturization, due to their unique properties and enhanced performance characteristics, making them excellent for detecting a wide variety of target substances with enormous precision. However, the design and optimization of nanostructured sensors involves significant challenges in exploring the parameter space and capturing complex parameter interactions. Several variables significantly affect the sensitivity of these sensors, which requires identification of the optimal combination of variables and their levels to improve sensitivity [Zhang-23], [Karimi-Maleh-23]. In this thesis, an approach based on response surface methodology (RSM) is proposed to aim these challenges and optimize the design of nanostructured sensors. RSM offers a statistical framework for efficient optimization of design parameters and allows consideration of multiple factors, complex interactions and maximizes sensor performance.

The objective of this thesis was oriented to explore and develop a data-driven approach for the optimal design of nanostructured sensors of high-specificity self-supported nickel nanowire arrays to detect hydrogen peroxide through applying a systematic and statistical methodology for the optimization of parameters based on the response surface methodology (RSM), managing to improve the sensitivity, selectivity, and general performance of these sensors. Besides, using RSM, it is possible to efficiently optimize the design of nanostructured sensors, reducing the number of sensors used in the study, lowering costs, decreasing the development times of the entire design, optimization, synthesis, and validation process in contrast to the limitations of traditional trial and error methods, as well as complicated multi-physics simulations, with high cost and computational processing time.

The existing problems in the development and optimization of nanostructured sensors imply challenges in the exploration of parameter space and the capture of complex parameter interactions. In contrast to simulations and traditional trial and error methods that are time

consuming and may not guarantee optimal results. Therefore, there is a need to develop a systematic approach based on experimental data to optimize the design of nanostructured sensors, considering multiple factors and their interactions.

The motivation behind this thesis arises from the desire to advance in the field of nanostructured sensors and overcome the limitations of traditional processes and simulations. Traditional trial and error methods can consume a lot of time and resources, with no guarantee of robust or successful results, while simulations can miss critical parameter interactions, as well as yield results that are unfeasible for real synthesis of such sensors. When applying RSM the motivation lies in the feasibility to improve the performance of these nanostructured sensors, which leads to higher sensitivity, selectivity, and reliability. The proposed approach offers a promising path for the design and development of efficient and reliable nanostructured sensors with enhanced performance characteristics.

The justification for this thesis lies in the need for a systematic and efficient approach to optimize the design of nanostructured sensors. Traditional methods, which involve changing one variable or factor at a time while holding all others constant to assess their impact on sensor response [Cheraghi-21], [Buledi-22], do not address potential interactions between variables that can affect sensor performance. Furthermore, this approach requires a lot of time and numerous experiments to identify the critical factors and their optimal levels [Montgomery-17]. Consequently, an alternative method is required that can simultaneously explain the interactions between multiple factors and optimize the sensor response. Multiphysics and multiscale simulations are other approaches to optimize sensor performance. These techniques describe coupled physical processes using partial differential equations (PDE) that interact simultaneously across several domains to produce the studied phenomena [Musa-12], such as the electrochemical theory of Dickinson *et al*. [Dickinson-14]. Finite element methods are typically used to generate numerical solutions for static geometries stable because closed-form solutions for these PDEs are generally not available [Musa-12], [Dickinson-14]. However, the computational complexity of this approach increases as the number of interactions increases, and the analysis becomes more detailed, making it computationally unfeasible and requiring substantial computational resources [Musa-12]. Moreover, the application of this approach to optimize the behavior of nanostructured sensors may be limited by the availability of efficient computational resources and the ability of software to generate high-precision solutions [Myers-16]. Therefore, exploring alternative

methods to improve the performance of nanostructured sensors is of paramount importance. Response Surface Methodology (RSM) has gained significant recognition in industry and academia for its effectiveness in identifying the optimal combination of variable levels while accounting for potential interactions between factors [Chan-19], [Box-87], [Box-92], [Viveros-Wacher-16]. RSM provides a statistical methodology that allows exploration of the parameter space, identification of influencing factors, and optimization of sensor design.

This thesis presents an application of RSM to design nanostructured sensors using an approach based on experimental data of self-supporting nanowire (Ni NW) arrays. Hydrogen peroxide (H_2O_2) was selected as the target molecule due to its wide applications in the clinical, pharmaceutical, and food industries [López-Cárdenas-21d], [Chen-12], [Cui-08], [Zong-17], [Satish-14], [Olarte-13]. In the clinical context, H_2O_2 is particularly vital as a surrogate molecule for sensing glucose levels, as it is a by-product of glucose catalysis by the enzyme glucose oxidase [Zong-17].

For the comprehension of linear models, the statistics *p* or *p-value* and r square (R^2) are defined as: the statistical values of *p* or *p*-value and *r* squared, which are used for the interpretation of linear models. The statistic *p* or *p*-value is the probability of obtaining a similar value by random. If $p < 0.05$ only means that, by convention, the null hypothesis (H_0) is unlikely to be true, so we reject it, although always with a small probability of being wrong. On the other hand, if $p > 0.05$ it is not guaranteed that H_0 is true since there may be a real effect and the study does not have enough power to detect it.

R square (R^2) indicates the variation in the data explained by the relationship between an independent variable and a dependent variable. The R^2 value varies from 0 to 1 and is expressed as a percentage.

Initially, a linear model fitted to the Ni growth data relating the length of the NW array to the electrodeposition time was established. An electrochemical growth rate was achieved like 0.97 μm/min ($p < 0.01$, 95% confidence interval (CI) [0.89, 1.06]) with an R^2 of 0.99, indicating a robust linear correlation between the two variables [López-Cardenas-22a], [López-Cardenas-23b]. This linear model served as a crucial foundation for understanding the influence of the electrodeposition time on NW growth, which was indispensable for optimizing the response of nanostructured sensors. Moreover, thorough statistical analyses were carried out to confirm the accuracy and validity of these findings for ensuring the reproducibility of the results. The high R^2

value obtained in this thesis demonstrated strong correlation between the electrodeposition time and NW length, which was critical for the accurate modeling and optimization of nanostructured sensors.

Subsequently, the general RSM problem is formulated and applied to optimize the response of a self-supported Ni NW matrix sensor based on a design variable and two variable levels as test condition. This approach was adopted because the response of the sensor is based on the design variable and the levels of the variables on which the measurements are made; therefore, both must vary simultaneously during the optimization process [Montgomery-17].

The length of the nanowires (Ni NW) was selected as the design variable, while the H_2O_2 concentration and the applied potential were treated as measurement variables, whose values were varied. Cyclic voltammetry (CV) was used for the characterization of the sensors [López-Cárdenas-21b]. A sensor that meets the theoretical requirements of optimal RSM design was also fabricated, and its response was compared with planar Ni and non-optimal nanostructured sensors. From the model, the optimal response region was experimentally identified: an optimal H_2O_2 concentration of 3.25 mM with a range of [0.34, 4.74] mM, an optimal length of 2.64 μm with a range of [0.68, 3.62] μm, and an optimal potential of 0.02 V with a range of [-0.0867, 0.0867] V. Finally, the optimal Ni NW sensor made with a length of 2.62 μm with a 95% CI of [2.48, 2.76] μm and showed a sensitivity to H_2O_2 of 3.55 mA/ (mM cm^2) with a limit of detection (LOD) of 0.78 mM H_2O_2 and a limit of quantification (LOQ) of 2.6 mM H_2O_2. These values indicated a significant improvement compared to a planar sensor (planar Ni with a length of 0 μm) with a sensitivity of 0.1 mA/(mM cm^2), a LOD of 0.95 mM H_2O_2, and a LOQ of 3.17 mM H_2O_2, as well as a non-optimal Ni NW sensor (with a length of 0.68 μm) with an H_2O_2 sensitivity of 1.55 mA/(mM cm^2), a LOD of 0.81 mM H_2O_2, and a LOQ of 2.71 mM H_2O_2. [López-Cárdenas-23b].

Through implementing RSM in the design of a Ni NW sensor for H_2O_2 detection, our goal is to highlight the advantages of employing data-driven strategies to optimize sensor performance, thus providing a valuable contribution to the field of nanostructured sensor design and enabling its practical use in a wide range of applications, benefiting the society.

Furthermore, this thesis describes in different chapters the application of a methodology for designing and developing low-cost, high-sensitivity nanostructured sensors to detect hydrogen peroxide H_2O_2 at different concentrations using well-known statistical tools.

A Brief Primer on Sensors Chapter 1, talks about sensors and some types of sensors, such

as electrochemical sensors, and biosensors, mentions some varieties of nanostructures, alludes to the development of nanowires by electrochemical synthesis, talks about nickel and some of its properties, finally, briefly mentions some of the statistical techniques and methodologies used for data analysis and optimization.

In Chapter 2, the methodology is presented subdivided into two areas, but in three subsections: statistical methodologies and electrochemical methodologies, subdivided into electrochemical synthesis and electrochemical characterization. The first subsection describes the formal statistical methodologies for the design and optimization of sensors. The second subsection describes the methodology of the electrochemical synthesis of nanostructures, and in the third subsection, the electrochemical characterization using cyclic voltammetry is described. During the development of research and experimentation of this thesis, some methodologies were implemented simultaneously, mixing the experimental part with the statistical analysis. In Methodology section too, the fabrication of nanostructured sensors by the process of nano structuration with nanowires by electrodeposition of nickel ions on membranes is described. Three variables as proof of concept were focused: nanowires length, measuring potential, and hydrogen peroxide concentration. Likewise, how the measurements were carried out with some nanostructured sensor prototypes using cyclic voltammetry (CV) is specified. The set of statistical tools of the DoE is explained, where systematically search in the experimental space combining the values of the design variables. Furthermore, the general RSM process that leads to the optimal combination of design variables is detailed.

In Data Analysis section, the data processing and statistical analyzes performed are described.

Moreover, in Results and Discussion section, the main outcomes obtained from the analysis of the design of experiments, as well as from the optimization using RSM are described, and in the Discussion, the scope of this study is delimited, indicating future directions.

Likely, in General Conclusions, the results are interpreted and compared with the results of the literature.

By combining in this thesis, the principles of nanostructured sensors, electrochemical synthesis, electrochemical characterization, statistical modeling, and data analysis, it was possible to optimize the sensitivity to hydrogen peroxide of nickel nanowire sensors. The outcomes will contribute to advancing sensor technologies, enabling improved detection capabilities, and

potentially impacting fields requiring accurate hydrogen peroxide measurements. In the same way, in the medical-clinical area, the detection and monitoring of glucose are due to the significant interrelationship of these two molecules, glucose and hydrogen peroxide.

.

1. A Brief Primer on Sensors

A sensor is a device or component that detects and responds to a stimulus or change in its physical environment. Its main function is to convert the physical or chemical magnitude it is designed to measure into some suitable physical response (mechanical, electrical, etc.), that can be processed and used by other systems.

Sensors are used in a wide variety of applications across different industries, ranging from automotive and aerospace to medicine, robotics, security, and many other fields. Some common examples of sensors include temperature sensors, pressure sensors, light sensors, motion sensors, proximity sensors, humidity sensors, and electrochemical sensors.

In general, sensors consist of a sensitive element that interacts with the stimulus being measured, and a circuit or processing system that converts the signal generated by the sensitive element into a usable output. This output can be an analog or digital signal, depending on the type of sensor and the specific application.

1.1 Electrochemical Sensors

Electrochemical sensors are a specific type of sensor that utilize electrochemical principles to detect and measure the concentration of certain chemical compounds or gases. They are commonly used in applications such as environmental monitoring, industrial processes, healthcare, and gas detection.

Electrochemical sensors typically consist of four main components: a sensing electrode (working electrode (WE)), a reference electrode (RE), a counter electrode (CE) and an electrolyte. The sensing electrode is specifically designed to interact with the target analyte (Ni self -supported nanowires array sensor), while the reference electrode provides a stable reference potential, a counter electrode. The electrolyte serves as a medium for ion transport between the electrodes. And Target analyte or substance for sensing like hydrogen peroxide (H_2O_2), was used. Because H_2O_2 is a byproduct of several biochemical processes, like glucose catalysis by glucose oxidase,

it has been widely used as a target molecule to develop new monitoring methods.

The operation of an electrochemical sensor involves the chemical reaction between the target analyte and the sensing electrode, resulting in a measurable electrical signal. This signal can be either a current or a potential, which is proportional to the concentration of the analyte.

There are different types of electrochemical sensors, including:

1. Amperometric Sensors: Measure the current generated by an electrochemical reaction between the target analyte and the sensing electrode.
2. Potentiometric Sensors: Measure the potential difference between the sensing electrode and the reference electrode, which is related to the concentration of the analyte.
3. Conductometric Sensors: Measure the change in electrical conductivity of the electrolyte due to the presence of the analyte.

Electrochemical sensors offer several advantages, such as high sensitivity, selectivity, and low power consumption. They can be highly specific to a particular analyte and exhibit excellent long-term stability. Additionally, they can be miniaturized and integrated into portable devices for on-site or point-of-care applications.

1.2 Nanostructured Sensors

Sensors with planar geometry can be improved by studying the effects of varying their geometry and measurement conditions. The presence of nanostructures increased sensor sensitivity. Some examples of nanostructures are nano walls, nanotubes, nanowires, nanoclusters, nanorods, and nanoparticles [Jia-09], [Cai-18], [Zong-17], [Chen-13], [Araujo-15], [Grupta-17]. These are just a few examples, and there are many other types of sensors available for different applications.

The development of nanowires by the electrochemical synthesis method was chosen since the conditions for the growing of the nanowires are relatively simpler and more easily controllable. Self-supported nanowire arrays were fabricated using nano porous constraining membranes to assist the growth of nanowires by electrodeposition. Using the characteristics of commercial nano porous membranes with a known density and pore diameter allows it to have better control in the development of these nanostructures, since these membranes function as a template for growth. Another advantage when using these nano porous membranes can cover one side of them with a

metal, which will allow them to fix the nanowires and obtain a self-supporting nanowires array and the manufacture of nanostructured sensors.

Nickel was chosen for the development of the nanowires, as it has a wide variety of electrochemical properties. Nickel is relatively easy to electrodeposit, even in complex geometries or nanostructured forms. Its electrodeposition process can be carried out using simple electrolytes and deposition setups. This ease of electrodeposition facilitates the fabrication of nanostructured nickel materials with controlled morphology, size, and composition. There advantages make of nickel a favorable choice for electrochemical synthesis, enabling the production of nanostructured materials, electrodes, and coatings for various applications, including electrocatalysis, energy storage, sensors, and electronic devices. These advantages of using nickel in electrochemical synthesis for numerous applications, including the following: high electrical conductivity, wide potential window, corrosion resistance, availability, and cost-effectiveness, versatility in nano structuring, and compatibility with other materials.

Nickel possesses excellent electrical conductivity, making it an ideal material for electrochemical processes. Its high conductivity enables efficient electron transfer during electrodeposition, leading to improved electrochemical performance and enhanced efficiency in electrochemical synthesis. Moreover, nickel exhibits a wide potential window, meaning it can operate over a broad range of potentials without undergoing significant electrode reactions. This property allows for versatile electrochemical processes, including electrodeposition, electroplating, and electrocatalysis, making nickel suitable for various applications. Furthermore, nickel demonstrates good corrosion resistance, particularly in aqueous environments. This resistance to corrosion helps ensure the stability and longevity of electrochemically synthesized nickel-based structures, making them suitable for long-term use in different conditions. In addition, nickel is widely available and relatively cost-effective compared to other metals. Its abundance in the crust of the Earth and its widespread industrial use contribute to its accessibility and affordability. This availability makes nickel a practical choice for large-scale electrochemical synthesis applications.

Other characteristics of nickel, include its versatility to be processed into various nanostructured forms, including nanowires, nanoparticles, and thin films. This versatility in nano structuring allows for the fabrication of tailored nanostructured materials with specific properties and applications. Nanostructured nickel can exhibit enhanced surface area, improved catalytic

activity, and unique physical and chemical properties beneficial for electrochemical synthesis. Besides, nickel demonstrates compatibility with a wide range of materials, making it suitable for integration and hybridization with other elements or compounds. This compatibility allows for the development of composite or hybrid materials with enhanced functionalities, such as improved conductivity, catalytic activity, or stability.

1.3 Biosensors

A biosensor is a device that combines a biological recognition element (such as enzymes, antibodies, or DNA) with a physicochemical transducer to convert a natural response into a measurable signal. Biosensors are designed to detect and quantify specific target analytes, such as biomolecules, chemicals, or pathogens, by exploiting the highly selective interactions between the biological recognition element and the target analyte [Rahman-19], [Cheraghi-21], [Bauer-22].

The critical components of a biosensor include are the biological recognition element, the transducer, the signal amplification and processing, and the output and display.

The biological recognition element of a biosensor can be classified into two main classes: biocatalysts (enzymes, tissues, etc.) and bioligands (antibodies, nucleic acids, lectins, etc.). The function of this biological recognition element is to bind to the target analyte of interest selectively. It can be a biological molecule, such as an enzyme, antibody, nucleic acid, or a whole cell, that exhibits specific binding affinity or catalytic activity towards the target analyte. The transducer converts the biological response or interaction between the recognition element and the analyte into a measurable signal. Depending on the specific detection principle employed, this can be an electrochemical, optical, piezoelectric, or thermal transducer. The biosensor may incorporate mechanisms for signal amplification or signal processing to enhance the sensitivity and accuracy of the detected signal. This can involve signal amplification through enzymatic reactions, nanomaterials, or signal enhancement techniques. Besides, the biosensor provides an output signal corresponding to the target concentration substance or presence. This output can be displayed or recorded for further analysis or interpretation.

Biosensors find applications in various fields, including medical diagnostics, environmental monitoring, food safety, agriculture, and industrial process control. They offer several advantages, such as high specificity, sensitivity, rapid response, portability, and real-time

monitoring capabilities. Biosensors enable on-site, point-of-care testing, improving disease diagnosis, enhancing food quality control, and facilitating environmental monitoring and safety assessments.

Overall, biosensors provide a powerful tool for sensitive and selective detection of target analytes, enabling various applications in different industries and sectors.

To turn a nanostructured sensor into a biosensor by relating the target molecules hydrogen peroxide and glucose, an enzyme called glucose oxidase (GOx) would have to be attached to the nanowires.

Glucose oxidase (GOx) catalyzes the oxidation of glucose, resulting in the production of gluconic acid and hydrogen peroxide. The hydrogen peroxide generated acts as a mediator, and its electrochemical detection in glucose biosensors provides a measurable signal that can correlate with the glucose concentration in the sample. This relationship forms the basis for the ability of the biosensor to detect glucose and quantify glucose levels in various applications, such as medical diagnostics and glucose monitoring in diabetes management [Liu-15], [Oliver-09].

Hydrogen peroxide (H_2O_2), glucose, and glucose oxidase (GOx) are interconnected in a biochemical pathway fundamental to the operation of glucose biosensors. Here is a schematic representation of their relationship:

Glucose Oxidation by Glucose Oxidase (GOx):

Glucose + O_2 → Gluconic Acid + H_2O_2

In this reaction, glucose oxidase (GOx) catalyzes glucose oxidation using molecular oxygen (O_2) as a co-substrate. As a result, gluconic acid is produced along with hydrogen peroxide (H_2O_2) as a byproduct.

H_2O_2 Detection in Glucose Biosensors:

H_2O_2 + Electrode → Electrochemical Signal

In glucose biosensors, the generated hydrogen peroxide acts as a redox mediator. It diffuses to the electrode surface, where it undergoes an electrochemical reaction. This reaction generates an electrochemical signal that can be measured and correlated with the glucose concentration in the sample.

Glucose Detection in Glucose Biosensors:

Electrochemical Signal → Glucose Concentration

The electrochemical signal obtained from the hydrogen peroxide detection is then converted into a quantifiable value, typically through calibration using known glucose concentrations. This calibration curve establishes the relationship between the detected signal and glucose concentration in the sample.

1.4 Optimizing Sensors by Numerical Techniques

Nanotechnology is a new and emerging science for developing nanostructured sensors. Methodologies such DoE and RSM, have not yet had a significant application impact in these areas.

There are some common statistical methodologies that researchers may employ to optimize the sensitivity of electrochemical sensors: design of experiments (DoE), regression analysis, analysis of variance (ANOVA), principal component analysis (PCA), sensitivity analysis, and optimization algorithms. These are just a few examples of statistical methodologies that researchers may employ to optimize. In this thesis the following statistical methodologies to enhance the performance of the sensor were used: design of experiments, response surface methodology, and in data analysis techniques were applied: linear modeling and bootstrapping. The bootstrap is a statistical resampling technique used for the interval estimation of point estimates.

DoE [Montgomery-17] and RSM methodologies provide an alternative to systematically exploring the space of variables with minimal experiments and at a low cost.

Most studies with the same objective are based on two main approaches, as briefly described below.

One of these strategies frequently explores the experimental space in a non-optimal way, one design variable at a time, which consumes time and money. Based on Multiphysics simulations, the other strategy is mathematically complex and computationally intractable [Goyal-20], [Qiao-12], [Musa-12], [Dickinson-14].

2. Methodology

This chapter describes the standardization of Ni growth by electrodeposition with linear model and bootstrapping, the experimental design used according to the statistical tools of design of experiments (DoE), using a 2^k factorial design, central composite circumscribed design and response surface methodology (RSM) and its principles, and the cyclic voltammetry (CV) characterization for data collection.

2.1 Statistical Methodologies: Design of Experiments, 2^k Design, Circumscribed Central Composite Design, and Response Surface Methodology

In this subsection, the methodologies applied as statistical methods are described to define a design of experiments (DoE) working with one design variable and two variables as the testing conditions to identify the experimental workspace from actual experimental data. In addition, starting with a simple design such as the 2^k design, in this case, 2^3 design, and adding four central points, one for each variable, and another one for the initially generated space, identifying the existence firstly of a linear behavior, getting a first-order model, after taking the slope steepest ascent. After several repetitions of those experiments, when observing a non-linear behavior due to the curvature found, a CCC design is applied to find the response surface identifying a theoretical maximum response point for those conditions (the optimal conditions). All these statistical methodologies will be described in the next subsections.

2.1.1 Design of Experiments (DoE)

The design of experiments is a powerful tool frequently used to research, design, develop, improve, and verify different processes, products, or devices in research and at an industrial level. DoE was used in this thesis because it allows knowing how many sensors are required and what

features must be evaluated and modified to evaluate them. The response variable was defined as the sensitivity response of the sensors in the presence of H_2O_2. Considering the high costs of experimentation, the need to work with real devices and in a limited study or research time. In this thesis, the design of experiments (DoE) and RSM methodology were used. DoE defined how many sensors and what dimensions these nanostructured sensors should have to achieve a response surface (RSM) that allowed knowing the optimal theoretical conditions with the smallest number of sensors [López-Cárdenas-22c].

Accurate designs require knowledge of sensor behavior in such electrochemical processes, leading to complex and complicated models. Managing these components frequently generates complex mathematical representations that are inconvenient for the calculation and the need for model validation. Hence, it is opportune to consider other approaches based directly on the experimental data, representing inputs and outputs of the system and adjustable design variables. Therefore, sensor performance is often summed up in several statistics in the empirical literature. Data obtained by CV was employed [López-Cárdenas-22b]. The DoE design was developed to evaluate the hydrogen peroxide sensitivity response of the sensor considering different concentrations in mM H_2O_2, the length of the nanowire sensors in micrometers (μm), and the potential in volts (V) [López-Cárdenas-22c], [López-Cárdenas-21e].

Whenever some process variables are intentionally modified in a DoE, it is possible to observe specific changes in one or more response variables of interest to study. These changes are convenient to make to evaluate all possible effects between the variables and their interactions. Statistically, DoE is an excellent method that allows experiments to be planned so that the data generated can be analyzed and objective conclusions can be obtained [Croarkin-12], [Lawson-14], [Gutierrez-Pulido-12], [Kyprioti-20].

On the other hand, the DoE is a viable methodology, to generate knowledge of the process or the system through careful planning of tests. DoE offers several statistical and engineering techniques for the adequate understanding of cause-effect situations [López-Cárdenas-23a].

A DoE begins by defining the objectives of an experiment and selecting the process factors to study. Adequate planning of concrete experimental works is required. If it is set a good design of experiments, this allows for obtaining relevant information with a particular punctual and specific work without being too extensive.

An appropriate planning process of the experiment based on a statistical design of

experiments is of the utmost importance so that adequate data is collected and analyzed by statistical techniques, obtaining valid and objective conclusions. There are two aspects to experimental problems: the design of the experiment and the statistical analysis of the data. Both points are interrelated because the analysis method depends directly on the procedure [Croarkin-12], [Montgomery-17], [Lawson-14].

2.1.1.1 Identifying and Selecting the Study Variables

Different characteristics or design variables were evaluated variables related to the system and the variables of electrochemical methods for synthesis and characterization. Firstly, the nickel ions metal was selected for developing the nanostructured sensors by electrochemical synthesis, as previous studies developed in the laboratory [López-Cárdenas-21a], [Alcalá-21], [Wasserman-04]. Second, the geometry of the nanostructures chosen by the self-support nanowires array sensors or thin films (planar sensors) was a significant variable, and they were obtained by electrodeposition [López-Cárdenas-21d], [López-Cárdenas-21c]. The thirst variable analyzed was the length of nanowires (NW).

Why is it so important to know the growth rate of nanowires?

Knowing the growth rate of nanostructures, including nanowires, is essential for controlling their dimensions, optimizing growth conditions, ensuring predictability and reproducibility, designing functional devices, and advancing fundamental understanding. It allows researchers to tailor the synthesis process to achieve desired properties and characteristics, facilitating the development of efficient and reliable nanostructured materials and devices for a wide range of applications.

The specific method chosen to determine the growth rate of nanowires depends on factors such as the growth technique, the properties of the nanowires, and the available characterization tools. The combination of different techniques and methods provides a more comprehensive understanding of the growth kinetics and allows for accurate determination of the growth rate.

Overall, by employing experimental techniques, real-time monitoring, and growth rate modeling, knowledge of these elements facilitates investigating and measuring the growth rate of nanowires, enabling precise control and optimization of their synthesis for various applications.

2.1.1.2 Preliminaries: Bootstrap a Resampling Method Characteristics

The bootstrap belongs to a class of statistical tools called resampling methods. These methods share three basic steps [Good-13], [Chihara-18], [Efron-86], [López-Cárdenas-21f]:

1) Repeatedly (re)sampling (with or without replacement) from a dataset.

2) Computing a statistic from the new sample (a subset of the original).

3) Compute the summary statistics (for example, measures of variation).

The resampling methods are often conceptually more straightforward and accurate than the asymptotic approximation methods and require fewer assumptions [Good-13]. Other resampling methods include permutation tests for hypothesis testing, cross-validation for model assessment, and model selection based on the model performance [James-13]. This thesis used the bootstrap to obtain measures of accuracy of estimates, i.e., interval estimation [Calin-Jageman-19], [Geng-13], [López-Cárdenas-21a], [Van-Beers-08], with linear regression, for the following purposes:

a) Calculate the average length of the nanowires of the sensors using ImageJ [López-Cárdenas-23b], [Abràmoff-04]. In Subsubsection 2.1.1.2.

b) Determine the confidence intervals for the Limit of Determination (LOD) and the Limit of Quantification (LOQ) [López-Cárdenas-21a], [López-Cardens-21f], this explanation will be described in Subsection 2.3.5.

c) Define the optimal measurement potential with a confidence margin of the CVs in the cyclic voltammograms [López-Cárdenas-21a], [López-Cárdenas-21d], this explanation can be seen in the Subsection 2.3.4.

d) Determine the sensitivity to hydrogen peroxide of the sensors with their confidence intervals. [López-Cárdenas-21a]. See Subsection 2.3.4.

In this thesis, interval estimates were considered 95% confidence intervals (CI) of the bootstrap percentile for point estimates and hypothesis testing. The *p*-values with a significance level $\alpha = 0.05$ was used.

The significance level (α) was considered like the probability of rejecting the null hypothesis when it is true. For example, a significance level of 0.05 indicates a 5% risk of concluding that there is a difference when there is no difference.

The statistic *p* or *p*-value is the probability of obtaining a similar value by random. If $p <$

0.05 only means that, by convention, the null hypothesis (H_0) is unlikely to be true, so we reject it, although always with a small probability of being wrong. On the other hand, if $p > 0.05$ it is not guaranteed that H_0 is true since there may be a real effect and the study does not have enough power to detect it. The significance level, also denoted as alpha or α, is the probability of rejecting the null hypothesis when it is true. For example, a significance level of 0.05 indicates a 5% risk of concluding that there is a difference when, in fact, there is no difference.

Here bootstrapping is used to obtain the length of the nanowires of the sensors. Those lengths were acquired from the scanning electron microscope (SEM) micrographs, shown in Fig. 2.1. ImageJ program was employed as a measurement tool in Fig. 2.1.

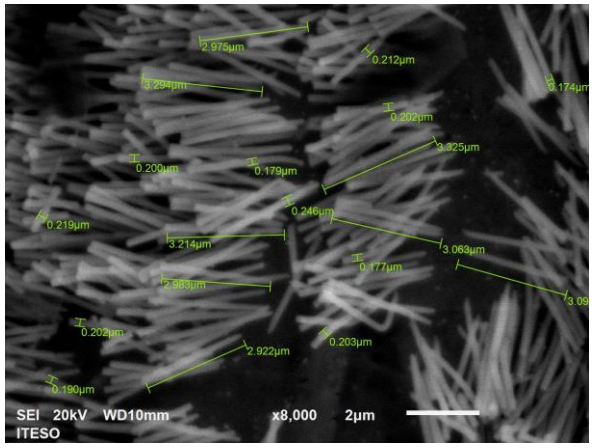

Fig. 2.1. Measurement of nanowire lengths using SEM pictures with ImageJ.

ImageJ was used to take about ten or more measurements of NWs lengths and computed the average length to make a scatter plot of the data [Armbruster-08], shown in Table 2.1. Bootstrapping was employed as described to calculate confidence intervals to have better approximate the NW lengths at 95 % CI of the desired length.

TABLE 2.1. ELECTRODEPOSITION TIME AND LENGTHS

Electrodeposition time (min)	Average Length (µm)
0.5	0.67
0.6	0.472
1.0	1.04
1.3	1.11
2.14	2.16
2.23	1.932
2.23	2.048
3.0	2.92
3.5	3.446
4.0	3.94

The relationship between the nanowires electrodeposition time and the resultant nanowires length experimentally obtained is shown in Table 2.1.

2.1.1.3 The Linear Model and the Rate Growing of the Nickel Nanowires

To obtain a growth curve of nanowires and determine the growth rate, data is typically collected through experimental measurements at different time intervals during the nanowire growth process. The data collection process requires the following steps: experimental setup, sample collection, characterization techniques, data analysis, and growth rate calculations.

An additional point of interest in this thesis was obtaining a curve of the growth length of nickel nanowires concerning electrodeposition time. Its calibration is important in the electrochemical synthesis of nanostructured sensors with nickel nanowires for several reasons: understanding growth kinetics, optimizing the fabrication process, calibrating growth parameters, enhancing sensor performance and sensitivity, and ensuring reliability and reproducibility [López-Cárdenas-21f], [Hocking-03a].

The growth length of nanowires, particularly nickel nanowires, is influenced by electrodeposition time, applied potential, electrolyte composition, and temperature. Understanding the growth kinetics of these nanowires is vital for sensor fabrication. By analyzing the relationship between electrodeposition time and nanowire length, it's possible to determine the optimal deposition time, ensuring consistent and reproducible fabrication. This calibration reference also helps standardize the fabrication process and enhances sensor performance, sensitivity, and response characteristics. Controlling nanowire length improves reliability and reproducibility, essential for implementing and commercializing nanostructured sensors.

The experimental setup involves the electrochemical synthesis of nanowires by electrodeposition. The growth parameters, and reaction time, are controlled and adjusted according to the desired growth conditions. These samples can be obtained by interrupting the growth process at specific time points. The collected samples are then characterized using appropriate techniques to determine the length or dimensions of the nanowires [Abràmoff-04]. Characterization techniques include scanning electron microscopy (SEM). The measured length or dimensions of the nanowires from each sample are recorded. The data is then plotted as a function of growth time

or duration, creating a growth curve. The growth curve represents the change in nanowire length or dimensions over time and provides insights into the growth kinetics. The growth rate can be determined from the growth curve by analyzing the slope of the curve at different time points. The growth rate represents the rate at which the nanowires increase in length or dimensions per unit time. It is typically expressed in terms of nanometers per minute. Statistical analysis can be applied to the collected data to assess the reliability and significance of the growth rate determination using a bootstrapping. After collecting data on the growth of the nanowires, a growth curve was constructed, and the growth rate was calculated. The growth curve and growth rate information are valuable for understanding the growth kinetics, optimizing growth conditions, and designing nanowires with desired dimensions for specific applications.

A linear model fitted to the Ni growth data relating the length of the NW arrays to the electrodeposition time was established. An electrochemical growth rate of 0.97 μm/min ($p < 0.01$, 95% confidence interval (CI) [0.89, 1.06]) was achieved, with an R^2 of 0.99, indicating a robust linear correlation between the two variables [López-Cárdenas-21f]. This linear model served as a crucial foundation for understanding the influence of the electrodeposition time on NW growth, which was indispensable for optimizing the response of nanostructured sensors [López-Cárdenas-21a]. Moreover, thorough statistical analyses were conducted to confirm the accuracy and validity of the findings and to ensure the reproducibility of the results. The high R^2 value obtained in this study demonstrated a strong correlation between the electrodeposition time and NW length, which was critical for the accurate modeling and optimization of nanostructured sensors [López-Cárdenas-21f]].

Likewise, the calibration curve of the growth rate of the Ni NW was obtained in a standardized way, shown in Fig. 2.2.

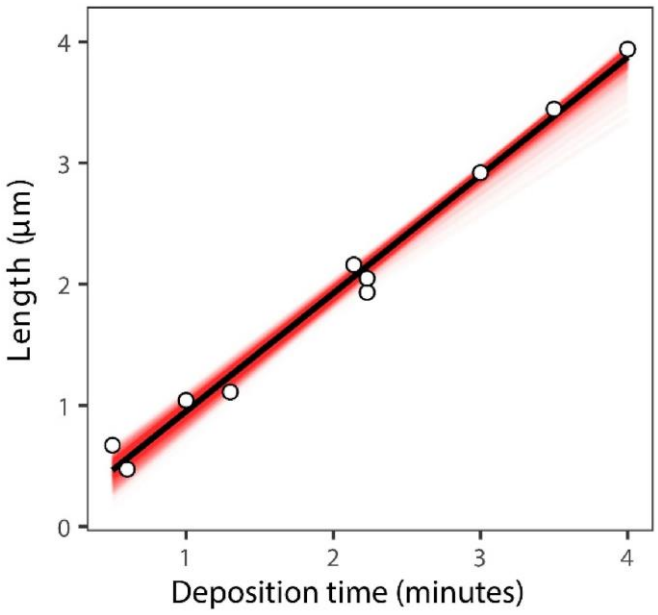

Fig. 2.2. Ni nanowires growth as a function of the electrodeposition time in PCTE membranes.

2.1.1.4 Polycarbonate Nanopores Membranes as Restrictive Template

The type of membrane material was used as a restrictive template with polycarbonate (PCTE), whose pore density is $4x10^8$, and the pore diameter size is Ø 100 nm. The thickness of such membranes is 6 µm [López-Cárdenas-21b], [López-Cárdenas-23b]. Fig. 2.3 shows a photo of PCTE nanopores membrane, before metallization.

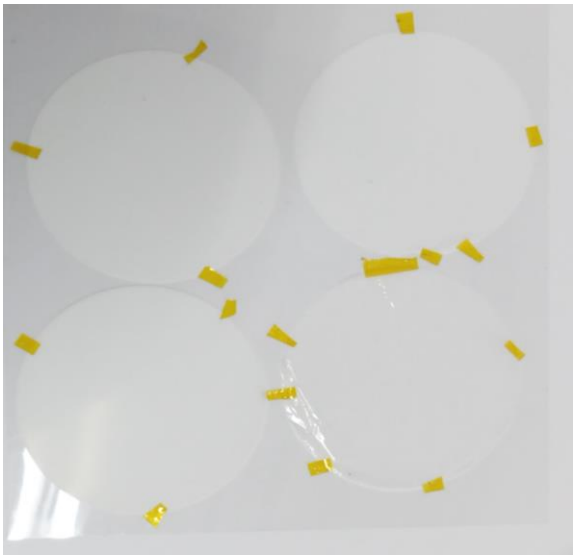

Fig. 2.3. Photo of nanopores polycarbonate (PCTE) membranes before metallization.

2.1.2 2^k Design

A 2^k design is a systematic and efficient approach to study the effects of multiple factors and their interactions. It allows to explore the factor space comprehensively and provides valuable insights into the factors influencing the response variable. The design is widely used in experimental research and statistical analysis to optimize processes, improve product quality, and make informed decisions based on the study of factor effects. The notation 2^k specifies that there are two levels (typically high and low) for each of the *k* factors being studied.

The design gets its name from the fact that it systematically explores all possible combinations of the factor levels.

The first step in this process is to start with an uncomplicated design to fit a first-order model of the form:

$$\mathbf{y} = \mathbf{x}\boldsymbol{\beta} + \boldsymbol{\varepsilon} \tag{2-1}$$

where **y** is the response matrix, **x** is the $k \times 2$ design matrix of coded variables with k rows from $i = 1$ to k factors, with the first column of **1** and the second column of factors. $\boldsymbol{\beta} = (\beta_1, \ldots, \beta_k)$ is the vector the coefficients of the model, for which we test the null hypothesis H_0: $\boldsymbol{\beta} = \mathbf{0}$, and ε is the source of irreducible variability, like measurement error.

For which the null hypothesis H_0: $\beta = 0$ was evaluated. For efficiency, beginning with a simple 2^k design is the usual, with two levels for each 1,2, …, k factors. If we obtain results suggest a linear response, we move towards the direction of the β coefficients of the first order model, that is, the direction of the steepest ascent. For regression analysis, and to evaluate the adequacy of the first order model, it is recommended to add n_c center points on which the treatments are $x_k = 0$, an addition that allows computing the experimental error [Myers-16], [López-Cárdenas-22c].

For illustration, without loss of generality, suppose we have an experiment with only two factors, x_1, and x_2, in coded variables. Next, it proceeds to choose sensible values of the natural variables and then augment the design with four center points. ($n_c = 4$).

Subsequently, the hypothesis that $\beta = 0$ is evaluated, and the lack-of-fit of the first order model. Suppose the lack-of-fit is verified. If the lack-of-fit is non-significant, and if the results suggest that the first order model is a good approximation (for example, plotting the response variable as a function of each natural variable and obtaining an almost linear response). When the linear behavior is not observed, another experiment is designed with new values of variables in the direction of improvement, that is, in the direction of the steepest ascent [López-Cárdenas-23b].

The equation (2-1) will be continuous using in the following sections 2.1.3.4

2.1.2.1 Describing and Developing Design of Experiments by 2^k Design

Before RSM, it is essential to find the region where the response was optimal with only the essential factors. Screening experiments are best suited for this exploration phase. Screening experiments make it possible to approach the region of optimality (the curvature) without using more levels than necessary.

The experiment started at 2^k design to keep the number of levels minimum. The number of levels is 2 and the number factors is $k = 3$ The selected factors are length of nanowires (factor

A), hydrogen peroxide (H_2O_2) concentration (factor B), and potential measurement (factor C). As shown in Fig. 2.4.

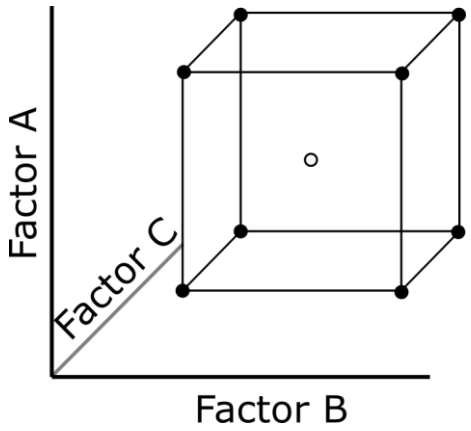

Fig. 2.4. Scheme of the designs of the experiment, the number of levels is 2 and the number factors is k = 3 The selected factors are length of nanowires (factor A), hydrogen peroxide concentration (factor B), and potential measurement (factor C).

2.1.2.2 Using and Applying Design of Experiments by 2^3 Design

Table 2.2 contains the design 2^3 with the treatments of factors.

Levels were coded as – and + for low and high values respectively, as indicated in the treatment column of Table 2.2. To estimate experimental error and ensure linearity, the design was augmented by a third point, a center point level, coded as 0 for all factors [López-Cárdenas-22c].

TABLE 2.2. DESIGNS OF EXPERIMENTS STARTING WITH 2^K FOR $K=3$ FACTORS IN THE NEXT DISTRIBUTION

Run	A	*B*	*C*	*Treatment*	*Replicates*
1	+	+	+	A high, B high, C high	3
2	-	+	+	A low, B high, C high	3
3	+	-	+	A high, B low, C high	3
4	-	-	+	A low, B low, C high	3
5	+	+	-	A high, B high, C low	3
6	-	+	-	A low, B high, C low	3
7	+	-	-	A high, B low, C low	3
8	-	-	-	A low, B low, C low	3
9-12	0	0	0	A center, B center	4

Table 2.3 shows: The levels of all the factors: the length of nanowires, the hydrogen peroxide concentration, and the potential, including also, the center points. [López-Cárdenas 2023b], López-Cárdenas 2022c], [Games 2013].

TABLE 2.3. STARTED DOE WITH 2^3 ASSINGING FACTORS: FACTOR A (LENGTH), FACTOR B (H_2O_2 CONCENTRATION), AND FACTOR C (POTENTIAL) WITH EACH LEVELS VALUES

Factors		*Levels*	
A	Length	+	3 µm
		-	1.3 µm
		0 (center point)	2.15µm
B	H_2O_2 Concentration	+	3.81 mM
		-	1.27 mM
		0 (center point)	2.54 mM
C	Potential	+	0.05 V
		-	-0.05 V
		0 (center point)	0 V

Table 2.4 shows the total number of sensors for 2^3 design, which is five (two lengths and two H_2O_2 concentrations, plus the center point). Note that even with the center point augmentation, this was still a 2^3 design [Montgomery-17], [Croarkin-12], [Lawson-14].

TABLE 2.4. IN DOE 2^3 SELECTING CHARACTERISTICS OF THE NI NW SENSORS USED

Sensors	*Length – H_2O_2 concentration*
1	3 μm – 3.81 mM
2	3 μm – 1.27 mM
3	1.3 μm – 3.81 mM
4	1.3 μm – 1.27 mM
5	2.15 μm – 2.54 mM

2.1.3 Circumscribed Central Composite Design (CCC)

From the Central Composite designs, the Circumscribed (CCC) was chosen. The design variable selected is the length of the nanowires, as system variables the measurement variables such as hydrogen peroxide concentration and potential measurement. Because the porous density turned out to be a constant per membrane, we ruled out the possibility of using the Box-Behnken method.

2.1.3.1 Schema of a CCC Design

A schematic representation of a CCC design is shown in Fig. 2.5. Starting with a 2^k hypothetical using $k = 2$ with an augmented center point (0,0), shown in Fig. 2.5 part (a), to better exemplify the process. If we augment the axial points (black stars), presented in Fig. 2.5 (b), they are obtained by rotating the basic layout 2^k. All axial points are at a distance α from the center. In

Fig. 2.5 (c), we can observe a factorial design by a 2^3 design cube augmented with axials points representing the CCC design, showing the region of the experimental space and the steepest ascent process. The curvature at which the maximum response can be reached by sequentially performing 2^3 layouts until the first-order model can no longer account for the data and detected quadratic effects [Myers-16], [Gutierrez-Pulido-12].

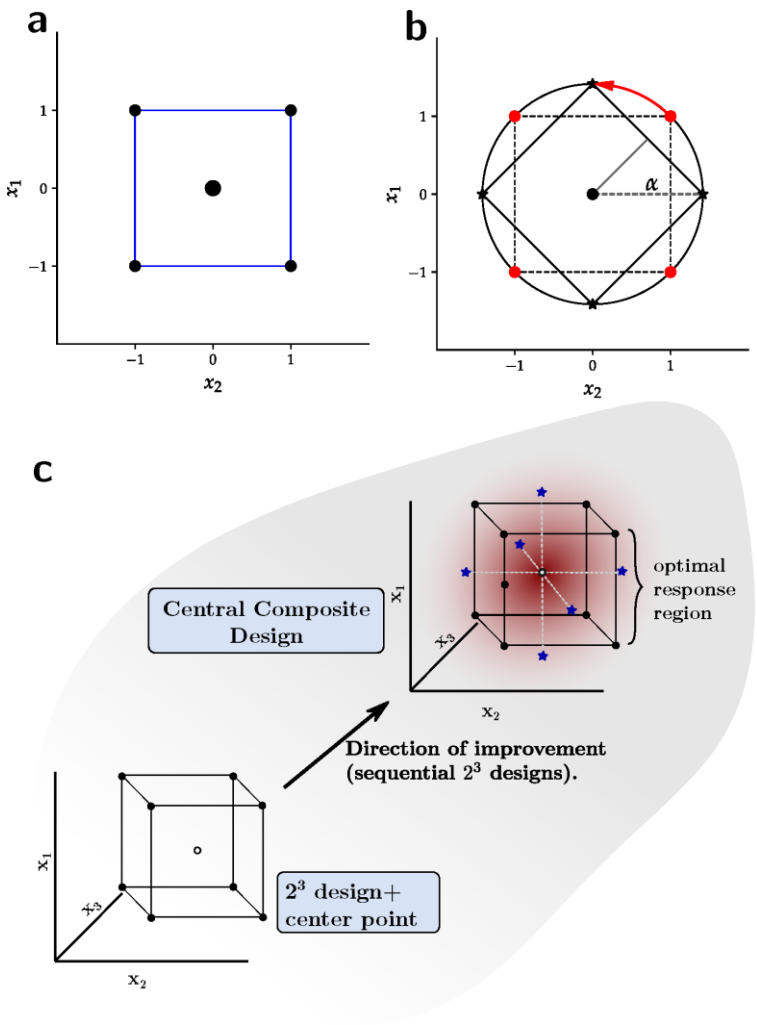

Fig. 2.5. Representation of experimental designs with two factors and the method of steepest ascent. (a): 2^k design with $k=2$, augmented a center point at (0,0). (b): Axial points (black stars) are obtained by rotating the basic 2^k design. All axial points are at α distance from the center. (c): Experimental space region and the process of steepest ascent with k =3. The curvature at which the response is maximum can be reached by sequentially performing 2^k designs until the first-order model can no longer account for the data and quadratic effects are detected.

The 2^k design process was repeated until there was evidence that the first-order model was not a good approximation and is complemented with a curvature test.

Suppose we conclude that quadratic effects cannot be rejected. The first-order model cannot be applied when this situation is achieved, and the steepest ascent method should be stopped [Montgomery-17], [Myers-16], [López-Cárdenas- 23b]. The application of the CCC design continues, and with RSM an optimal quadratic model is obtained. It will be described in the subsection 2.1.3.6.

2.1.3.2 Formulating RSM by Description of CCC Design

In RSM we model the response *y* as

$$y = f(\boldsymbol{\xi_1}, \boldsymbol{\xi_2}, \dots, \boldsymbol{\xi_n}) + \varepsilon \tag{2-2}$$

where *f* is unknown, but it can approximate it; $\boldsymbol{\xi_1}, \boldsymbol{\xi_2}, \dots, \boldsymbol{\xi_n}$ are the variables (often called natural variables in the RSM jargon) upon which the response y depends, and ε is the source of irreducible variability, like measurement error. It will assume ε is distributed normally with mean zero and variance σ^2. The expected value of *y* is thus:

$$E[y] = E[\, f(\boldsymbol{\xi_1}, \boldsymbol{\xi_2}, \dots, \boldsymbol{\xi_n})] \tag{2-3}$$

2.1.3.3 Codification of Natural Variables

Because the variables ξ_i can have different units, it is advisable to transform the variables with feature scaling for to make easier the analysis and comparison in a common scale. The most common scaling is the linear transformation:

$$x = (b - a)\frac{\xi - \xi_{min}}{\xi_{max} - \xi_{min}} + a \tag{2-4}$$

where *x* is the encoded variable, *a* and *b* correspond to the minimum and maximum values of *x*, that is, $x_1 = x_{min} = a$, and $x_2 = x_{max} = b$. Furthermore, ξ_{min} and ξ_{max} represent respectively the

minimum and maximum of the real values of the original variables.

For *x*, the coded variable falls in the range of [*a*, *b*]. If we want $x \epsilon$ [-1,1] centered at zero, then the transformation becomes:

$$x = \frac{\xi - [\xi_{max} + \xi_{min}]/2}{[\xi_{max} - \xi_{min}]/2} \quad (2\text{-}5)$$

The original variables range of [*a*, *b*] were equivalent to [low, high]. It used the interval [−1, 1] centered at zero for the coded variable. The coded variables using the transformation (2-5) are shown in Table 2.5.

TABLE 2.5. DOE 2^3 WITH THE VALUES OF THE ORIGINAL VARIABLES AND THEIR CODED VALUES

Run	*Length μm*	*H_2O_2 concentration mM*	*Potential [V]*	x_1	x_2	x_3
1	1.3	1.27	-0.05	-1	-1	-1
2	3	1.27	-0.05	1	-1	-1
3	1.3	3.81	-0.05	-1	1	-1
4	3	3.81	-0.05	1	1	-1
5	1.3	1.27	0.05	-1	-1	1
6	3	1.27	0.05	1	-1	1
7	1.3	3.81	0.05	-1	1	1
8	3	3.81	0.05	1	1	1
9	2.15	2.54	0	0	0	0
10	2.15	2.54	0	0	0	0
11	2.15	2.54	0	0	0	0
12	2.15	2.54	0	0	0	0

2.1.3.4 Starting the RSM Process

The RSM process is illustrated in Fig. 2.5 (a)-(c). The first step in this process is to start with an uncomplicated design to fit a first order model of the form like la equation (2-1).

We proceed first by choosing sensible values of the natural variables ξ_1 and ξ_2, and then augment the design with n_c = 4 center points. After conducting the experiment, it fit the model of equation (2-1), we can find the estimates of the coefficients in:

$$\hat{\mathbf{y}} = \mathbf{x}\,\widehat{\boldsymbol{\beta}} \tag{2-6}$$

where $\hat{\mathbf{y}}$ is the estimate response matrix, **x** is the matrix of coded variables with *k* rows from *i* = 1 to *k* factors, with the first column of **1** and the second column of factors**.** $\widehat{\boldsymbol{\beta}} = \left(\hat{\beta}_1, \ldots, \hat{\beta}_k\right)$ are the estimated coefficient of the model. We then tested the hypothesis that $\beta = \mathbf{0}$, and test the lack-of-fit of the first order model.

2.1.3.5 The Method of Steepest Ascent

If the lack-of-fit is non-significant, and the results suggest that the first order model is a good approximation (for example, plotting the response variable as a function of each natural variable and obtaining an almost linear response), it proceeds to design another experiment with new variable values in the direction of improvement. These new values can be obtained using the coefficients as follows (for x_1):

$$\Delta x_1 = \frac{\beta_1}{\beta_2}\Delta x_2 \tag{2-7}$$

Then convert Δx_1 to the natural variable ξ_1. This process is repeated until there is evidence that the first order model is not a good approximation and complemented with a test of curvature.

2.1.3.6 Testing Curvature with Second-order Model

The test of curvature can be obtained using a *F*-test with the sum of squares of pure quadratic ($SS_{quad.}$) and the mean squared (pure) error (MSE) [Montgomery-17], [Myers-16], [López-Cárdenas-23b]. The MSE can be computed as

$$MSE = \frac{\sum_{j=1}^{n_c}(y_j - \overline{y}_c)}{n_c - 1} \tag{2-8}$$

where y_j is the values of the center points, the $\overline{y}_c$ is the mean of the values center points, and n_c is the total number of center points.

and the SS_{quad}. with

$$SS_{quad.} = \frac{n_f n_c(\overline{y}_f - \overline{y}_c)}{n_f + n_c} \tag{2-9}$$

where $\overline{y}_f$ and $\overline{y}_c$ are the mean response for the factorial and center points, respectively, in addition n_f and n_c are the total number of the factorial and center points correspondingly.

The test is performed with the F_α statistic at some α level of significance (explained in Subsubsection 2.1.1.2), with $F = SS_{quad}./MSE$ and n_c - 1 error degrees of freedom. If, for example, $n_c = 4$ and $\alpha = 0.05$, the $F_{0.05} = 10.13$. So that any value of F below 10.13 is rejected, in which case it concludes that quadratic effects cannot be rejected. When this situation is achieved, the first order model cannot be applied, and the method of steepest ascent should stop [Montgomery-17], [Myers-16], [López-Cárdenas-23b]. However, for a quadratic model to be applied, it needs more data points to estimate the terms of equation (2-10), which requires that the main effects be not aliased, because the method of least-squares to solve equation (2-10) requires a full-rank matrix.

$$\mathbf{y} = \mathbf{x}\boldsymbol{\beta} + \mathbf{x}'\boldsymbol{\mathcal{B}}\mathbf{x} + \boldsymbol{\varepsilon}1 \tag{2-10}$$

where **y** is the response matrix, **x** is the matrix of coded variables, $\mathbf{x}'$, likewise $\boldsymbol{\beta}$ are the main effects coefficients as in equation (2-1), and $\boldsymbol{\mathcal{B}}$ is the $k \times k$ symmetric matrix.

(2-11)

[1] As with the first-order model, the estimates of the second-order model coefficients are $\hat{\beta}$ and $\hat{\boldsymbol{\mathcal{B}}}$, and the estimated response is thus $\hat{y}$.

$$\boldsymbol{\mathcal{B}} = \begin{bmatrix} \beta_{11} & \frac{1}{2}\beta_{12} & \cdots & \frac{1}{2}\beta_{1k} \\ & \beta_{22} & \cdots & \frac{1}{2}\beta_{2k} \\ & & \ddots & \beta_{kk} \end{bmatrix}$$

The quadratic terms x_{ij}^2 with $i = k$ have the diagonal coefficients of $\boldsymbol{\mathcal{B}}$, and the two-way interaction terms $x_i x_j$ with $i < j$ have coefficients that results of the sum of the off-diagonal terms, that is, when $\beta_{ij} = \beta_{ji}$, which becomes $\beta_{ij} x_i x_j$; **x** is the $k \times 2$ design matrix as in equation (2-1). This matrix $\boldsymbol{\mathcal{B}}$ (2-11) has a main diagonal whose values correspond to the coefficients of the quadratic terms (β_{kk}) and outside of the diagonal principal, in the triangular superior part and in the triangular inferior part there are not zeros, numbers are the half of the value of the interaction terms coefficients of ($\frac{1}{2}\beta_{1k}$).

The quadratic model has (k + 1) (k + 2)/2 terms, so it needs at least the same number of independent runs to estimate the coefficients. The estimation of $\boldsymbol{\beta}$ and $\boldsymbol{\mathcal{B}}$ is achieved by adding *axial* points to the 2^k design.

In the Fig. 2.5 (b) shows how it can add the axial (sometimes called *star*) points. If the square of the original 2^2 factorial design is rotated, the most extreme (*axial*) points are at α distance from the origin. (These axial points, also represented by the letter α, were explained in sub-subsection 2.1.3.1; they are different from the α that represents the significance level explained in sub-subsection 2.1.1.2). The axial point in this part, is the value of α here is just the radius of the unit circle. In terms of the square sides, α is the distance of hypotenuse of the right triangle formed by the center and the perpendicular bisector of the rotated square; hence $\alpha = \sqrt{1^2 + 1^2} = \sqrt{2}$. This can be generalized to the unit hypersphere as $\alpha = \sqrt{k}$ for k factors. The resulting optimal design is called spherical or Circumscribed Central Composite (CCC) design [Myers-16], [López-Cárdenas-23b], [Croarkin-12], [López-Cárdenas-22b].], with $2^k + 2k + 1$ independent runs, allowing to fit the second-order model.

Fig. 2.5 (a) - (c) shows experimental space region and the process of steepest ascent. The curvature at which the response is maximum can be reached by sequentially performing 2^k designs until the first order model cannot longer account for the data and quadratic effects are detected.

Fig. 2.5 (a) - (c) shows the sequential procedure for $k = 3$. As with the $k = 2$, we can start with a simple 2^k design augmented with center points and repeat this process until it cannot reject the presence of curvature (quadratic effects). Then it can use a CCC adding axial points to the original 2^k design, with the axial points with coordinates $(0, -\alpha, 0)$, $(-\alpha, 0, 0)$, $(0, \alpha, 0)$, $(\alpha, 0, 0)$, $(0, 0, -\alpha)$, and $(0,0, \alpha)$, with $\alpha = \sqrt{3}$. If the axial points are added after running the 2^k, the analysis should be done by blocking the first set of runs in Block 1 (points 1 to 12) shown in Table 2.5, and the second (added axial points since 13 to 18) in Block 2 [Montgomery-17], [Myers-16], [López-Cárdenas-23b], [Lawson-14]. Showed in Table 2.6.

TABLE 2.6. CIRCUMSCRIBED CENTRAL COMPOSITE DESIGN CCC WITH AXIAL POINTS IN THE SECOND BLOCK OF VALUES OF THE ORIGINAL VARIABLES AND THEIR EQUIVALENT CODED VARIABLES (CENTRAL COMPOSITE DESIGN WITH AXIAL POINTS. THE RUNS FROM 1-12 ARE OMITTED AS THEY ARE THE SAME AS IN TABLE 2.5)

Run	*Length* μm	H_2O_2 *concentration mM*	*Potential V*	x_1	x_2	x_3
13	0.68	2.54	0	-1.73	0	0
14	3.62	2.54	0	1.73	0	0
15	2.15	0.34	0	0	-1.73	0
16	2.15	4.74	0	0	1.73	0
17	2.15	2.54	-0.0867	0	0	-1.73
18	2.15	2.54	0.0867	0	0	1.73

2.1.3.7 Applying Response Surface Methodology (RSM)

RSM was applied to design nanostructured sensors from a data-driven approach using experimental data. Firstly, the general RSM problem was formulated. In previous subsections, 2.1.2 and 2.1.3 , all the Design of Experiments (DoE) processes necessary to obtain the RSM were described and developed. In addition, all the results obtained from the DoE were used to continue developing and applying the Response Surface Methodology. Finally, an RSM model was obtained, and the optimized theoretical conditions were found [López-Cárdenas-21e], [López-Cárdenas- 23b].

However, for a quadratic model to apply, you will need more data points to estimate the terms. This process will be continued in the Results section of Chapter 4.

2.2 Nanostructures Synthesis Methodology

In this chapter section, the electrochemical methodologies used like electrochemical synthesis or electrodeposition for the development of nanowires are described, as well as the electrochemical characterization using the cyclic voltammetry method for the measurement of said nanostructured sensors. Also, it mentions the equipment of nano porous membrane metallization. There are descriptions about the processes for these techniques were developed, and the supports used for the development and characterization (measurement) of the self-support nanowires arrays nanostructured sensors whose objective is to optimize their sensitivity to hydrogen peroxide.

2.2.1 Reagents and Materials

Hydrogen peroxide solution H_2O_2 (30 % w/w), sodium phosphate dibasic, (Na_2HPO_4, ACS reagent, ≥99.0%) and sodium phosphate monobasic, (NaH_2PO_4, ACS reagent, ≥99.0%), were obtained from Sigma-Aldrich. Deionized water, hydrochloric acid (HCl, 37%) and Sodium hydroxide (NaOH) flakes were purchased from Golden Bell and Jalmek, respectively. Ag pellets (99.99%) and Ti pellets (99.995%) were obtained from Kurt Lesker.

Nickel plating solution were obtained from Caswell Inc. All reagents were used without further purification. Polycarbonate track etched nano porous membranes, 47 mm in diameter, 0.1 μm pore size, pore density of $4x10^8$ pores/cm^2 and 0.6 μm thickness were obtained from STERLITECH. Colloidal Silver paint was purchased from Ted Pella. Commercial epoxy glue transparent, Resistol® strong repair, can be readily found [López-Cárdenas- 23a].

2.2.2 Synthesis and Characterization Equipment

For membrane metallization, an e-beam system INTERCOVAMEX TE12 was employed. Synthesis by electrodeposition was performed with a Keithley™ 2400 Source Meter Unit controlled with LabView software [Keitley-11]. A scanning electron microscope (SEM) JEOL JSM-6010LA was used at 20 kV acceleration voltage for morphological and chemical characterization and for the measurements of the lengths of the nanowires (shown in Table 2.1 and in Fig. 2.1. The scanning electron microscope (SEM) is a type of electron microscope capable of producing high-resolution images of the surface of a sample using electron-matter interactions. A potentiostat/galvanostat EC301 by Stanford Research Systems was used for electrochemical characterizations and H_2O_2 detections.

The CV setting used the scan rate at 100 mVs^{-1}, and a potential window of -0.6 V to 0.6 V. EC301 uses a free Windows software (SRSLab) to support all the primary electrochemical techniques, including voltammetry, and can be downloaded from the SRS web site. Data is acquired over the TCP/IP interface. In addition, the data is easily exported to spreadsheets and graphing packages.

2.2.3 Synthesis of Self-Supported Nanowires Arrays (Nanostructured Sensors)

The nanostructured electrodes of sensors consist of nickel self-supported nanowires array (Ni NW). Polycarbonate membranes were used as a restrictive nano porous membrane like templates to grow the Ni nanowires by electrodeposition, an electrochemical method [Nasirpouri-17], [López-Cárdenas-21b], [López-Cárdenas-21f], [López-Cárdenas-22a]. Before electrodeposition, one side of PCTE membranes was metalized with a silver (Ag) thin film by

physical vapor deposition. First, a 5 nm titanium (Ti) layer was evaporated at 0.6 Å/s to guarantee Ag adherence, and then 500 nm of Ag was evaporated at 2.1 Å/s. Shown in Fig. 2.6.

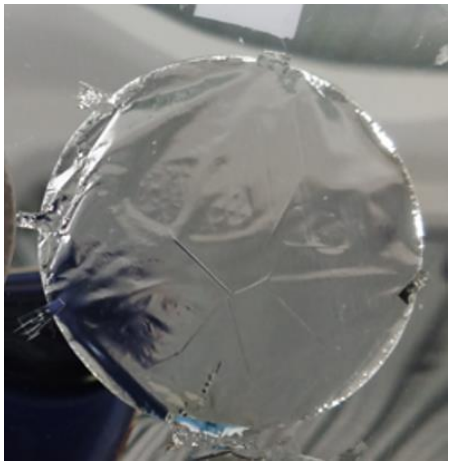

Fig. 2.6. Polycarbonate nano porous membrane metalized with silver (500 nm of Ag) photo.

Firstly, the materials for electrochemical synthesis were washed with hydrochloric acid HCl at 30% to be free of grease and contaminants. All the materials were dried with an air gun. The metalized membranes cut off the acetate. They were arranged in the system in the following order. It used a piece of acrylic as a support, with dimensions of 3x3x0.7 cm. A rectangular 4x2 cm piece of the copper metal sheet was put on the acrylic base. It worked like a current conductor to help a working electrode (WE). As well, putting the film membrane very carefully it will be electrodeposited, with the metallic face in contact with the copper sheet; on top, it placed a piece of rubber with a circular perforation to delimit the area to be electrodeposited on it the electrolytic cell was fixed with the help of two large butterfly clamps. It must be very well sealed so that the electrolyte solution is not spilled [López-Cárdenas-23b], [López-Cárdenas-22a]. It is shown in Fig. 2.7.

The electrochemical synthesis was performed in a typical three-electrode cell configuration. The electrodes used were a platinum (Pt) electrode of 3 mm diameter (eDAQ ET075) as the counter electrode (CE), a saturated silver-silver chloride (Ag/AgCl) electrode as

reference electrode (RE), and the working electrode (WE) was the metalized nano porous membrane in contact with a thin copper plate. Fig. 2.7 show two photos of experimental electrochemical synthesis [López-Cárdenas-21d].

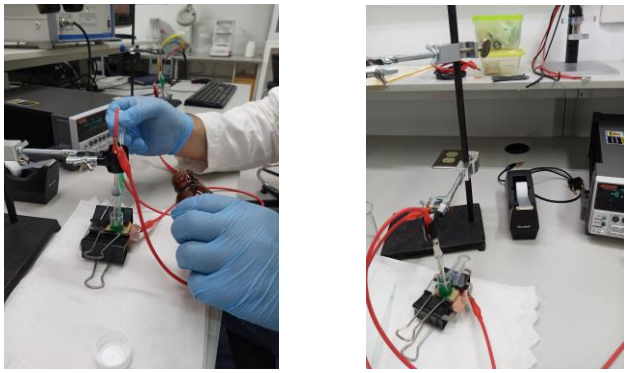

Fig. 2.7. Images of experimental electrochemical synthesis.

The electrolytic cell was conformed at the bottom of the cylinder, with a hole connecting the solution electrolyte with the membrane immersed, allowing the Ni ions to pass through the pores. The ions were electrodeposited using a constant potential of -1.1 V at different times. Fig. 2.8 shows is a schematic representation of Ni nanowires electrochemical growth process [López-Cárdenas-23b], [López-Cárdenas-22a].

A plot of the electrochemical synthesis process is shown in Fig. 2.8.

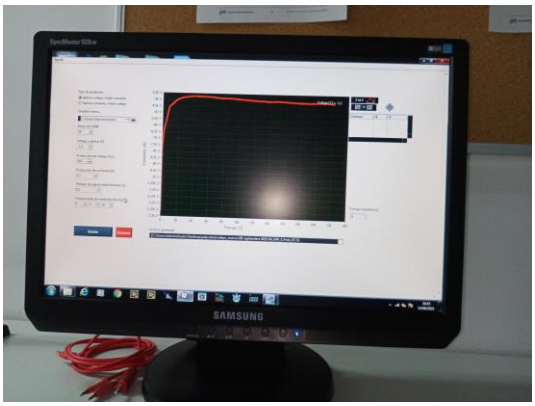

Fig. 2.8. Plot of Ni NW PCTE with 3.7 minutes of electrochemical synthesis process using -1.1 volts of potential applying.

The electrodeposition times range were varied from 0 to 4 minutes to obtain widely different lengths.

A representation of electrodeposition of Ni nanowires electrochemical growth process is shown in Fig. 2.9.

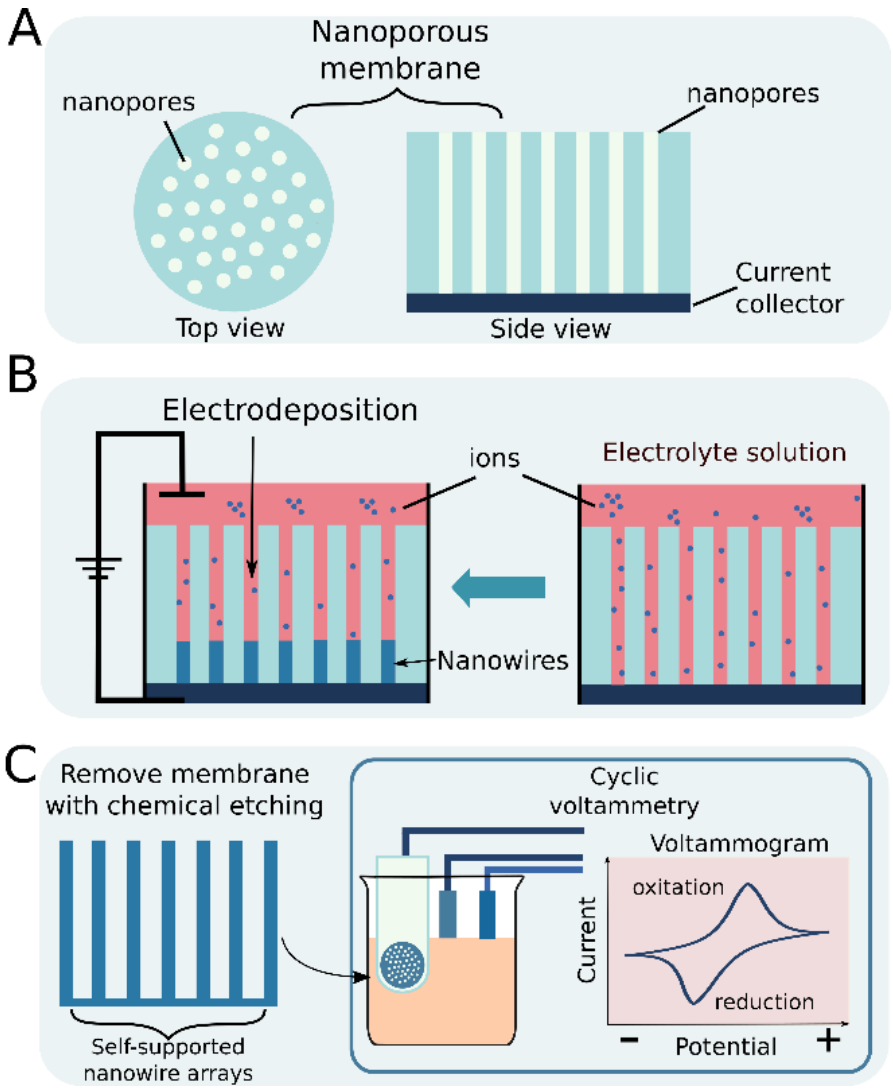

Fig. 2.9. Schematic representation of synthesis of self-supported nanowire arrays and collection data. A: Top and side views of the restrictive nano porous membranes used. Membrane pores are randomly distributed. B: Illustrative diagram of the electrodeposition process using the membranes in panel A. C: Self-supported nanowire arrays over the current collector (in the left). The process of data collection using CV is illustrated in the right. See sections 2.2 and 2.3.

After electrodeposition, the treatment for the self-supporting nanowires array was released by chemical etching. The Ni NW was immersed in 3M NaOH solution for cleaning, and the membrane was removed. Once the Ni NW was dry, a small sample was cut and sent to be observed by the SEM [López-Cárdenas-23b].

In SEM images, it was possible to measure the Ni NW lengths and verify their cleanliness. Fig. 2.10 shows some micrographs of Ni NW with different times of electrodeposition [Calin-Jageman-19], [López-Cárdenas-21d], [Nasirpouri-17], [Thomas-17].

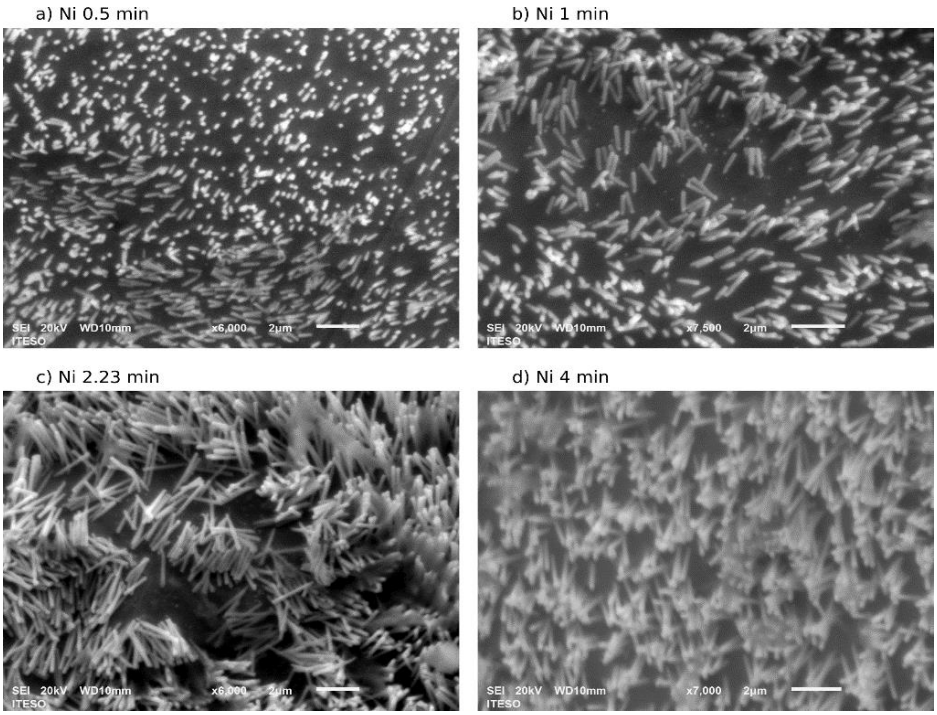

Fig. 2.10. Micrographs of nanowire arrays of Ni electrodeposited with different durations. The images were taken with a scanning electron microscope (SEM) JEOL JSM-6010LA in the ITESO facilities. a) with 0.5 min of electrodeposition, the nanowire lengths had a mean length of 0.67μm; b) with 1 min, the mean length was of 1.04μm; c) with 2.23 min, the mean length was of 2.05μm and d) with 4 min, the mean length was of 3.95μm.

The energy dispersive spectroscopy (EDS) technique performed in the SEM was mainly used for chemical characterization, analysis of materials, identification, and quantification of chemical substances present in detectable concentrations in the samples of the self-supported nickel nanowires arrays observed in the SEM [López-Cárdenas-22a], [Nasirpouri-17], as shown in Fig. 2.11.

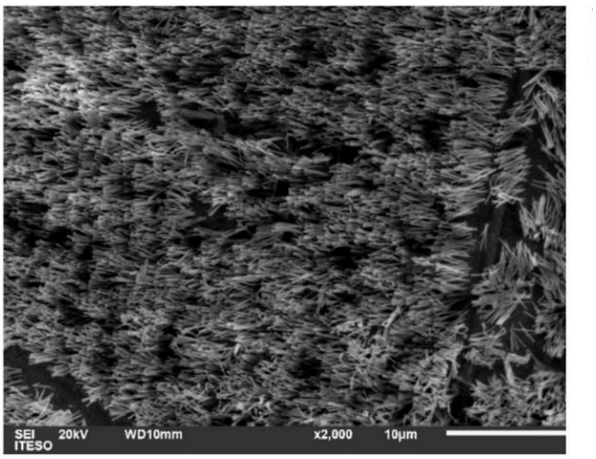

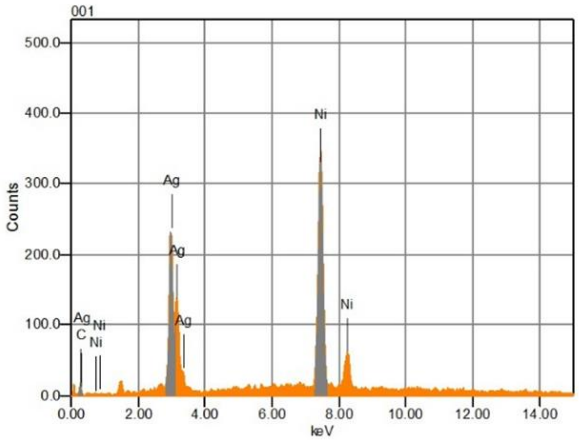

Chemical formula	ms%	mol%	Sigma	Net	K ratio	Line
C	3.60	17.21	0.14	310	0.0001269	K
Ni	70.45	68.96	0.46	24034	0.0602671	K
Ag	25.95	13.82	0.26	17669	0.0169645	L
Total	100.00	100.00				

Fig. 2.11 Elemental chemical characterization obtained by energy dispersive spectroscopy (EDS) from the SEM of Ni NW after PCTE membrane removal.

2.3 Electrochemical Characterization by Cyclic Voltammetry (CV)

Electrochemical characterization is an excellent technique used to study the behavior sensors and understand the importance of reaction mechanisms implicated like charge transfer, electrolyte transport, and electron transport [López-Cárdenas-21d], [López-Cárdenas-22b], [López-Cárdenas-23b], [Nasirpouri-17], [Hua-11], where multiphysics phenomena are involved.

2.3.1 Cyclic Voltammetry

Cyclic voltammetry (CV) is one of the methods of electrochemical characterization used to measure potential, current, and charge. Also, CV is used to identify and detect electrolyte concentrations or a chemical reactivity substance [López-Cárdenas-22b], [Chen-13].

Electrochemical characterization in an electrochemical cell depends on many factors, including the condition of the working electrode, counter electrode, the ions of the electrolyte solution, the current, the charge, and the potential. All of them are responsible for the oxide-reduction reaction changes. A scheme of cyclic voltammetry and a type of voltammogram are shown in Fig. 2.12.

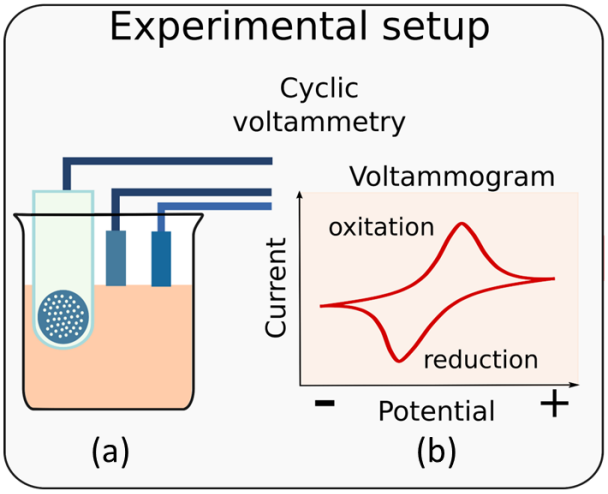

Fig. 2.12 Cyclic voltammetry process and data acquisition. a) Schematic of electrochemical characterization in a typical three-electrode cell configuration for the cyclic voltammetry (CV). b) A standard voltammogram generated by CV data acquisition computation.

The electric potential is measured between the reference electrode and the working electrode. In contrast, the auxiliary electrode closes the electric circuit. The potential of the working electrode is sensitive to the substance concentration. At the same time, the current flows through the counter and the working electrodes. The reference electrode was selected to avoid a polarizable behavior [López-Cárdenas-22b], [Chen-13], [Thomas-17]. Fig. 2.13 shows an electrochemical characterization, including a Ni NW nanostructured sensor and the nickel nanowires in a SEM micrograph.

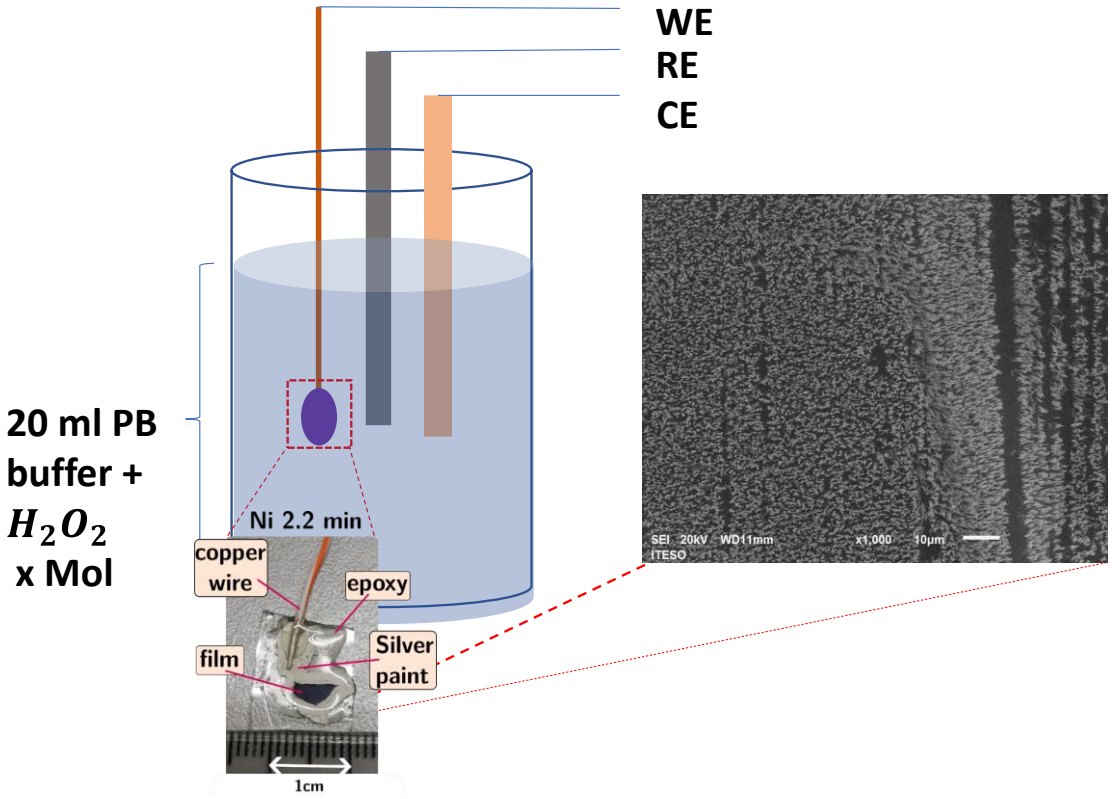

Fig. 2.13 Electrochemical characterization in a typical three-electrode cell. The working electrode (WE) is the nickel self-supported nanowires array with 2.2 minutes of electrodeposition time and a Ni NW SEM micrograph.

Since some years ago, nanotechnology has been used for developing nanostructured sensors, and many researchers have been interested in applying electrochemical methods for testing hydrogen peroxide (H_2O_2), using more sensitive and selective non-enzymatic sensors. [López-Cárdenas-23a], [Hua-11], [Thomas-17].

On the other hand, hydrogen peroxide is a common substance and has many uses in different industries: clinical laboratory, medical diagnostics, pharmaceutical, food processes, environmental, mining, textile industry, pulp, paper bleaching, antiseptic, disinfecting agents, beverage, cleaning products applications [López-Cárdenas-21b], [López-Cárdenas-21c], [López-Cárdenas-22b], [Cai-18].

The literature mentions the mechanism of electrochemical reduction for H_2O_2 in reducing of cathodic peak [Zong-17], [Chen-12], [Cai-18], [Rahman-19]. It can be represented in the following form:

$$H_2O_2 + e^- \rightarrow OH_{ad} + OH^-$$
$$OH_{ad} + e^- \rightarrow OH^-$$
$$2OH^- + 2H^+ \rightarrow 2H_2O$$

2.3.2 Electrochemical Characterization Measurements and Quantitative Detection of H_2O_2

The electrochemical sensors measurements were carried out using H_2O_2 at different concentrations in a phosphates buffer solution of 0.05M PB with pH = 7.0. The H_2O_2 concentrations employed were 0, 0.34, 0.5, 1.0, 1.5, 2.54, 3.25, 4.74 and 6.5 mM, utilizing a distinct container in each one. Solutions were prepared by directly adding the volume corresponding to the desired H_2O_2 concentration to a necessary volume of 0.05M PB solution, sufficient to obtain a total of 20 ml of the mixture for each of the different concentrations. One concentration was used independently for every CV measurement without stirring. After each H_2O_2 concentration was measured for five cycles, the electrodes were cleaned and rinsed with deionized water, removing the excess with anti-static Kimtech wipes. All experimental work was carried out at room temperature [López-Cárdenas-21b], [López-Cárdenas-23b].

2.3.3 Data Acquisition of the CV Measurements

The manufacturing characteristics of the sensor used in Fig. 2.14 were developed with restrictive nano porous membranes by electrodeposition of Ni ions (previously described in Subsections 2.2.3 and 2.3.1) [López-Cárdenas-21d], [López-Cárdenas-22b], [Musa -12], [Dickinson-14]. In these experiments, the information generated from the initial experimental designs was applied.

Fig. 2.14 shows seven cyclic voltammograms, characterizing a single Ni NW sensor with a nanowire length of 0.68 µm, detecting its response at seven different concentrations of hydrogen peroxide.

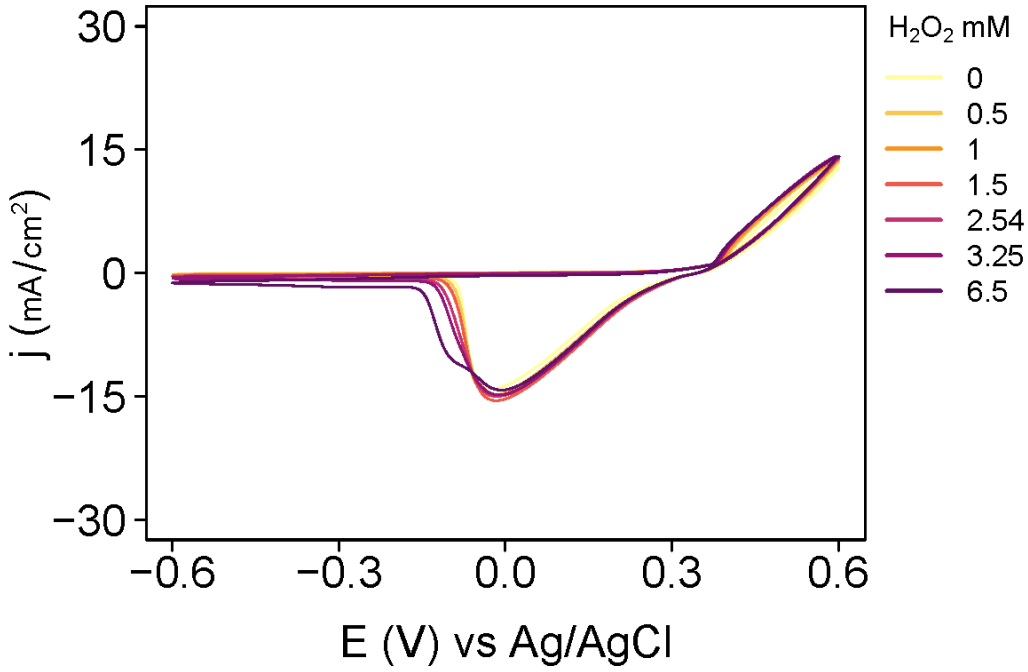

Fig. 2.14 Seven cyclic voltammograms of seven different concentrations of H_2O_2 obtained from a single chip by electrochemical characterization.

2.3.4 The Electrochemical Response (Current Intensity and Current Density)

The response current intensity was transformed to current density (I density, in mA/cm^2), dividing the current intensity by the sensor area. This thesis has been interested in the sensitivity of the sensor, which was defined as the change in current density by a unitary increment in H_2O_2 concentration, with dimensions mA/ (mM cm^2). Because the sensitivity critically depends on the

potential applied [López-Cárdenas-21b], [López-Cárdenas-23b], the potential V^* at which is maximized was identified. The process is as follows: in the reduction peak region of the CV (approximately from -0.6 V to 0.6 V), *I* density was interpolated for each of the *i*-th potential with a step size of 0.0005 V [Hayfield-08], [Rojo-Álvarez-18], [Paternoster-98], [Guideline-05]. All CVs were taken with each concentration by five cycles to get stabilization. Hence, for each $V[i]$ the pairs (*I* density $V[i]$, concentration$_s$) were obtained, for the $k = 7$ concentrations, where the intercept of the equation is represented by $\alpha_{V_{[i]}}$, and estimated the sensitivity of the sensor with the slope of the linear regression $\beta_{V_{[i]}} = \beta$ as follows:

$$I \text{ density}_{V_{[i]}} = \alpha_{V_{[i]}} + \beta_{V_{[i]}} * \text{ } H_2O_2 \text{ concentration} \tag{2-12}$$

The potential at which the sensitivity is maximized is, therefore,

$$\underset{V}{\text{argmax}} \ \beta = V^* \tag{2-13}$$

Using (2-12), the sensitivity was obtained for the Ni planar; it was β = 0.1 $\frac{mA}{mM\ cm^2}$, and for a Ni NW with length mean of 0.68 µm, the sensitivity was β =1.55 $\frac{mA}{mM\ cm^2}$

Fig. 2.15 shows the voltammograms (CVs) obtained with different concentrations in five different sensors with the following lengths: 0.68 µm, 1.3 µm, 2.15 µm, 3.0 µm, and 3.62 µm. These CVs allow us to observe the different responses or electrochemical characterizations of five Ni NW sensors.

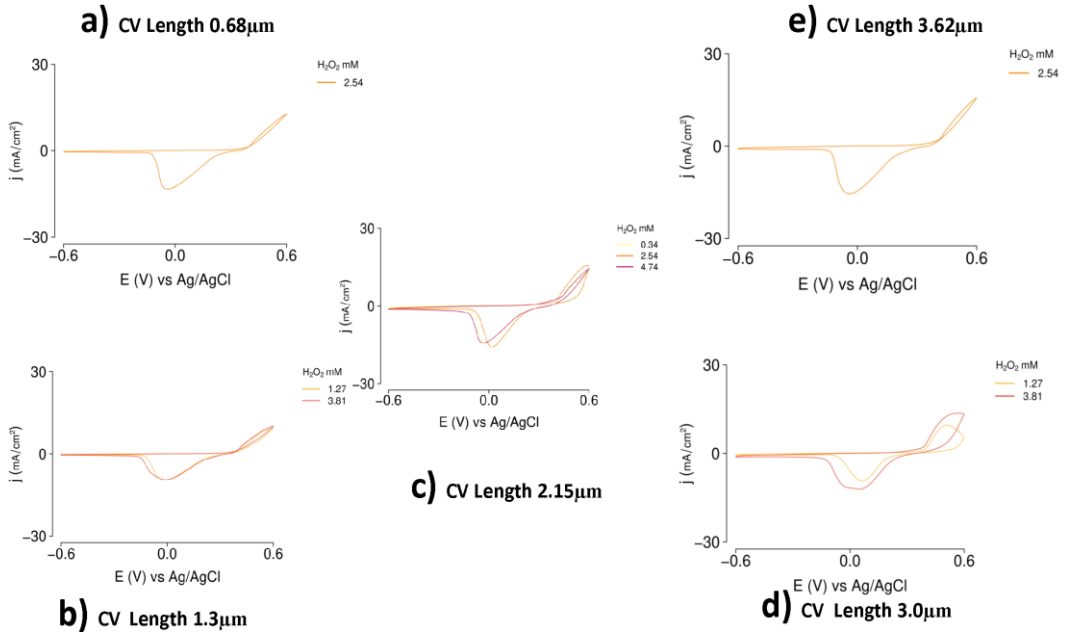

Fig. 2.15 Comparing CVs of different sensors with different concentrations.

Fig. 2.16 shows the seven voltammograms of each of the three Ni sensors, allowing us to observe their different responses.

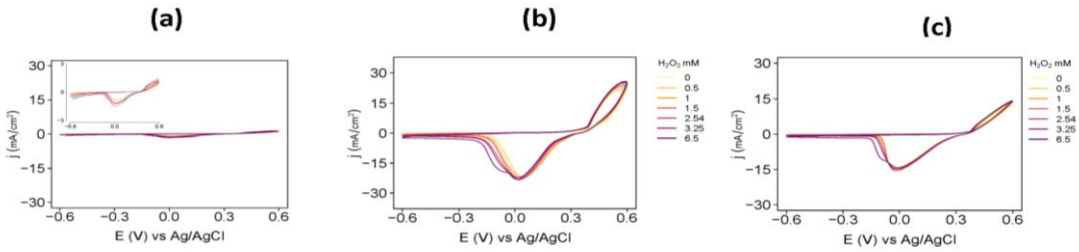

Fig. 2.16 Comparing CVs of three different sensors with the same seven concentrations, (a) Planar sensor with 0 µm of length. (b) Ni NW with 2.62 µm of length, and (c) Ni NW with 0.68 µm of length.

2.3.5 Limit of Detection (LOD), and Limited of Quantification (LOQ)

Limit of Detection (LOD) is the lowest concentration of a substance in a test sample that can be easily distinguished from zero [López-Cárdenas-21d], [Armbruster-08].

$$LOD = \frac{3*RSE}{\beta} \tag{2-14}$$

where, β is the slope of the linear regression with units mA/ (mM cm^2), and SE is the standard error of the β. The limit of detection (LOD) and the limit of quantification (LOQ), both in mM of H_2O_2, were obtained with (2-14) and (2-15), using RSE like the residual standard error.

Limit of Quantification (LOQ) is the lowest concentration of a substance in a test sample that can be determined with acceptable repeatability and precision.

$$LOQ = \frac{10*RSE}{\beta} \tag{2-15}$$

However, accurate designs require knowing most of the behavior present in the sensors, leading to complex and complicated models. Using those representations often presents drawbacks for computation and the need for model validation [López-Cárdenas-21b], [López-Cárdenas-22b], [Armbruster-08], [Guideline-05], [Paternoster-98].

Using (2-14) and (2-15), the LOD and LOQ values of two different nickel sensors were obtained: a nanostructured Ni sensor (Ni NW) with a length of 0.68 microns, its LOD = 0.81 and LOQ = 2.71 mM H_2O_2, while for the Ni planar sensor its LOD = 0.95 and LOQ = 3.17 mM H_2O_2, it is observed that the values that can be detected and quantified of hydrogen peroxide are lower with a Ni NW sensor than with a Ni planar sensor. The planar geometry was used as a reference

for the comparison of the response to H_2O_2 since it represents the most extreme case of a non-nanostructured sensor [López-Cárdenas-21b], [López-Cárdenas-21d]. These results were calculated from the data obtained by cyclic voltammetry to the hydrogen peroxide response in seven different concentrations: 0, 0.5, 1.0, 1.5, 2.54, 3.25, and 6. 5 mM H_2O_2.

3. Data Analysis Tools and Procedures

The raw CV was processed with customized R package [Lenth-20] or scripts. The fourth cycle was taken as it was the most stable of the five CV cycles run for each concentration and per manufactured sensor. From this, only the reduction peak corresponding to the lower semicircle of the cyclic voltammogram was analyzed, where the current intensity was measured negatively. This reduction peak was normally considered with a window potential between -0.25 to 0.25 volts. The current intensity was transformed into current density in milliamps per square centimeter, dividing the intensity by the sensor area. The sensor area was calculated by measuring its contour with a rule-scale and helping with a stereoscopic microscope.

For the 2^k experimental design, the R package *rsm* was used [Lenth-20]. With the data from the 2^k experimental design, linear models were fitted using ordinary least squares (OLS), and the evidence of curvature was evaluated with a Fisher Test (*F*-test) [López-Cárdenas-23b], [López-Cárdenas-22d]. This test of curvature can be obtained using an *F*-test with the sum of squares of pure quadratic $(SS_{quad.})$, and the mean squared (pure) error (MSE) [Montgomery-17], [Myers-16]. The MSE can be computed as *F*-test. See sub-sub-section 2.1.3.6 [López-Cárdenas-22d]. An extended quadratic model was adjusted to optimize the response (current density), also with the R package *rsm* [Lenth-20], [Lawson-14], [Good-13], [Chihara-18].

As mentioned in Chapter 1, the bootstrap is a statistical resampling technique used for the interval estimation of point estimates. The main idea is to simulate the sampling distribution variation by taking samples, with replacements, from the original data. A statistic of interest (like the slope of a linear regression model) is computed and stored for each resample. After B resamples, the resulting variation can be summarized with the lower and upper 95% percentile [Efron-86], [Löpez-Cárdenas-21f]. In almost all the analyses, one thousand resamples were used with reposition B=1000, except in the rate growing that was used B=250 [López-Cárdenas-21a].

The results of the statistical tests are evaluated with an alpha significance level of 0.05, and confidence intervals of 95% were obtained using the bootstrapping method. See Sub-subsection

2.1.1.2 [Efron-86], [López-Cárdenas-21f], [Good-13], [Chihara-18].

The lengths of nanowires were determined on the SEM images (as can be explained before in Sub-subsection 2.1.1.2) using ImageJ [Abràmoff-04] as shown in Fig. 2.1. Bootstrapping was employed to calculate confidence intervals to have better approximate the NW lengths at 95 % CI of the desired length.

ImageJ was used to take about ten or more measurements of NWs lengths and computed the average length to make a scatter plot of the data, as shown in Fig. 2.2.

In the same way, the rate growth with the bootstrapping technique was measured and obtained using Scanning Electron Microscope (SEM) micrographs.

The transformed data was smoothed using nonparametric regression with the R package *np* [Hayfield-08].

4. Results and Discussion

This chapter presents the results obtained throughout the optimization process of the self-supported nanowires array sensors employing RSM and DoE. In addition, the nanostructured development of sensors with the optimal theoretical conditions of the variables obtained in the RSM for validating the results, and a discussion.

4.1 Describing Results from Response Surface Methodology

This section presents some statistical processes for obtaining the RSM results, which are a continuation of those previously mentioned in Sub-subsection 2.1.3.7.

4.1.1 Processes Using the Response Surface Methodology

In this section, the different experimental designs applied, 2^k design, CCC, and RSM, are presented to get the optimal theoretical characteristics of the sensor to achieve its optimal sensitivity to hydrogen peroxide. [Myers-16], [Lenth-20], [Box-87], [Box-92], [López-Cárdenas-23b], [Cumming-05], [Cumming-13], [Cleveland-79].

4.1.2 Getting the Response Surface in a Factorial Design Augmented with Center Points.

This study continues from the results of the Table 2.5.

Based on previous findings, [López-Cárdenas-21b], [López-Cárdenas-21f], [Croarkin-12], [Lawson-14], [Gutierrez-Pulido-12], [Kyprioti-20], we start from the following 2^3 design, with H_2O_2 concentrations of 1.27 and 3.81 mM (low and high), lengths of 1.3 and 3 μm, and potential of -0.05 and 0.05 V. Four center points ($n_c = 4$) runs were added with 2.54 mM, 2.15 μm and 0 V. Shown in Table 2.5, Sub-subsection 2.1.3.3 it is called the Block 1 from 12 runs, with the naturals

and the coded variables. This process is repeated until there is evidence that the first order model is not a good approximation and is complemented with a curvature test [Lawson-14]. Explain Fig. 4.1 here.

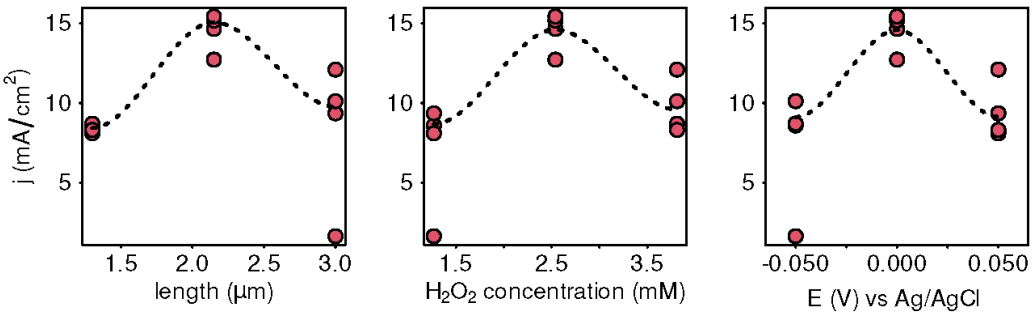

Fig. 4.1 Response as a function of length, H_2O_2 concentration and potential. In all cases, the response is evidently nonlinear. The line shows a fitted LOESS [locally estimated scatterplot smoothing; [Cleveland-79] regression to emphasize the nonlinearities of the relationship between the response and the independent variables.

As mentioned before, the response was normalized by the sensor area, so when it refers to the response of the sensor it means a density of current intensity, in units of mA/cm^2 [López-Cárdenas-23b],

The model was fitted from (2-1) using the *R* package *rsm* [Lenth-20], [Myers-16]. All the coefficients were non-significant (see Table 4.1), but the lack-of-fit (F (5, 3) = 18.27, $p < 0.05$) and curvature (F (1, 3) = 66.71, $p < 0.01$), using (2-8) and (2-9), were significant, suggesting quadratic effects. Furthermore, we plotted the response variable as a function of the factors levels and found that the response was nonlinear and possibly quadratic, as shown in Fig. 4.1.

TABLE 4.1. STATISTICAL SUMMARY OF THE FIRST ORDER MODEL WITHOUT INTERACTION TERMES

	Estimate	95% CI	t (8)	p-value
β_1	-0.062	[3.5, 3.37]	-0.041	> 0.05
β_2	1.44	[-2, 4.88]	0.97	> 0.05
β_3	1.1	[-2.33, 4.53]	0.74	> 0.05

4.1.3 Applying the Circumscribed Central Composite Design

After the fit to a linear model failed on the 2^3 design, the design was augmented with axial points to yield a CCC Design (see Fig. 2.5c); added axial points are shown in natural and coded variables in Table 2.5. With this design, a second-order model was fitted from on (2-10), with main effects $\beta_{12}x_1x_2$, $\beta_{13}x_1x_3$ and $\beta_{23}x_2x_3$; and quadratic terms $\beta_{11}x_1^2$, $\beta_{22}x_2^2$, and $\beta_{33}x_3^2$.

Table 4.2 presents the statistical results for the coefficients obtained by fitting the second-order model. The effects of the length and H_2O_2 concentration were non-significant; however, the effect of the potential was significant. The interactions length × concentration and length × potential also was non-significant, whereas concentration × potential was significant. All the quadratic terms were significant.

The ANOVA of the model showed significant joint first-order (linear) effects (F (3, 16) = 15.83, $p < 0.001$), two-way interactions (F (3, 16) = 4.16, $p < 0.05$ and quadratic effects (F (3, 16) = 35.31, $p < 0.001$). Overall, the model was statistically significant (F (10, 16) = 17.87, $p < 0.001$) [Hocking-03b], [Stahle-89], [Stahle-89], [López-Cárdenas-23b].

TABLE 4.2. STATISTICAL SUMMARY OF THE SECOND-ORDER MODEL

		Estimate	95% CI	*t* (14)	*p*-value
Main effects	β_1	0.22	[-0.71, 1.15]	0.50	> 0.05
	β_2	0.83	[-0.10, 1.76]	1.92	> 0.05
	β_3	2.10	[1.42, 2.78]	6.60	< 0.05
Interaction terms	β_{12}	1.36	[0.13, 2.59]	2.38	> 0.05
	β_{13}	1.32	[0.09, 2.55]	2.31	> 0.05
	β_{23}	-0.70	[-1.93, 0.53]	-1.23	< 0.05
Quadratic terms	β_{11}	-1.24	[-2.09, -0.40]	-3.15	< 0.05
	β_{22}	-1.23	[-2.07, -0388]	-3.11	< 0.05
	β_{33}	-3.61	[-4.36, -2.86]	-10.29	< 0.05

The sensor response ($\hat{y}$) is optimized where its partial derivatives are zero, $\frac{\partial \hat{y}}{\partial x_k} = 0$. This is achieved by differentiating (2-10) with respect to $\boldsymbol{x}$ and setting the result equal to $\mathbf{0}$. In matrix form we get (4-1)

$$\frac{\partial \hat{y}}{\partial \boldsymbol{x}} = \hat{\beta} + 2\widehat{\boldsymbol{B}}\boldsymbol{x} = \mathbf{0} \tag{4-1}$$

Solving for $\boldsymbol{x}$ we can find the *k* points at which the response can be optimal. Those points are given by

$$\boldsymbol{x}_0 = -0.5\widehat{\boldsymbol{B}}^{-1}\hat{\beta} \tag{4-2}$$

Now, it is unknown if this stationary point is a maximum, a minimum or a saddle point. To know this, we can find the eigenvalues of the matrix $\widehat{\boldsymbol{B}}$, which contains the coefficients of the two-way interaction and quadratic terms. The eigen decomposition of $\widehat{\boldsymbol{B}}$ into its eigenvalues and eigenvectors can be done as usual. Let **M** be the $k \times k$ matrix whose columns are the eigenvectors of $\widehat{\boldsymbol{B}}$ so

$$\widehat{\boldsymbol{B}}\mathbf{M} = \lambda\mathbf{M} \tag{4-3}$$

where λ are the eigenvalues of $\widehat{\boldsymbol{B}}$. Rearranging (4-3) $\left(\widehat{\boldsymbol{B}} - \lambda\mathbf{I}\right)\mathbf{M} = 0$ and using the determinant, the eigenvalues can be obtained by solving.

$$\left(\widehat{\boldsymbol{B}} - \lambda\mathbf{I}\right) = \mathbf{0} \tag{4-4}$$

From Table 4.2, we have the following matrix (symmetric) and vector.

$$\widehat{\boldsymbol{B}} = \begin{bmatrix} -1.24 & 0.68 & 0.66 \\ 0.68 & -1.23 & -0.35 \\ 0.66 & -0.35 & -3.61 \end{bmatrix}, \qquad \hat{\beta} = [0.22 \quad 0.83 \quad 2.10]$$

Therefore, using (4-2), the stationary point was $\mathbf{x}_0$ = [0.57, 0.56, 0.34] in coded variables, and ξ_0 = [2.64, 3.25, 0.02] in natural variables. To ensure that this point is a maximum, the eigenvalues must be negative, $\lambda_k < 0$ [Myers-16], [Lenth-20], [López-Cárdenas-23b], [Lawson-14]. Solving the (4-4), it was obtained λ_k = [−0.54, −1.66, −3.88], which allows to conclude there is a maximum at $\mathbf{x}_0$. Fig. 4.2 shows some contours and 3D plots of the surface just found. Having found the (theoretical) optimal conditions (length of 2.64 μm, at H_2O_2 concentration of 3.25 mM, measured at a sensing potential of 0.02 V).

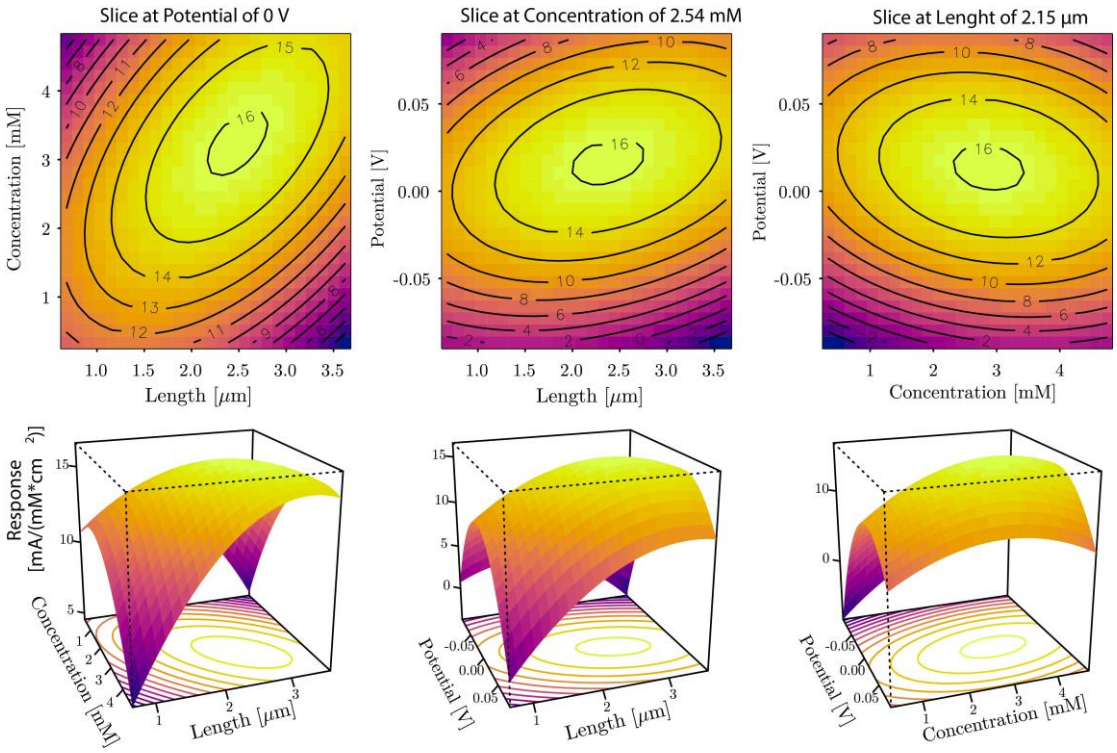

Fig. 4.2. Contours and perspective plots show the region at which the response reached the maximum (theoretical) response at the optimal length, concentration, and detection potential of 2.64 µm, 3.25 mM H_2O_2, and 0.02 V (natural variables), respectively.

The above theoretical values were obtained within the following ranges: for H_2O_2 concentration [0.34, 4.74] mM H_2O_2, for the length [0.68, 3.62] µm; and, for the potential [-0.0867, 0.0867] V [López-Cárdenas-22d].

4.2 Empirical Validation of the Optimal Design

After determining the (theoretical) optimal conditions (2.64 µm NW length, 3.25 mM H_2O_2

concentration, and 0.02 V sensing potential), a sensor with the optimal length was fabricated for further analysis and confirmation by electrodepositing Ni on PCTE membranes at different deposition times (between 2.6 and 3.5 min). The NW lengths of the sensors were measured using ImageJ software [Abràmoff-04]. The 95% CI for the mean length was computed using 1000 resamples for all the measured samples [Efron-86], [López-Cárdenas-21a], and then, the sample for which the 95% CI contained the desired length of 2.64 µm was selected. For the selected length, the mean length was 2.62 µm with a 95% CI [2.48, 2.76] µm and a min-max range of 2.1-3.3 µm. See Fig. 4.3.

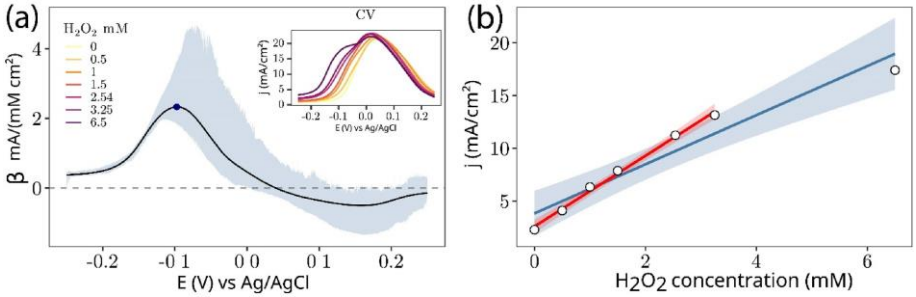

Fig. 4.3. Response of the optimized sensor measured by CV. (a) Sensitivity as a function of the applied potential in CV; the dot shows the potential at which the sensitivity is maximized. The inset shows the CV reduction peak region. (b) Regression plot of the response as a function of the H_2O_2 concentration. Note that above the concentration of 3.25 mM H_2O_2, the response decreases with respect to the expected trend (blue line). The second fit in red shows a better performance between 0 and 3.25 mM H_2O_2.

The desired length was 2.64 µm ∈ [2.48,2.76] µm. Fig. 4.4 shows micrographs of the optimal synthesized NW arrays, and the response to H_2O_2 of this sensor was characterized, see Fig. 4.3.

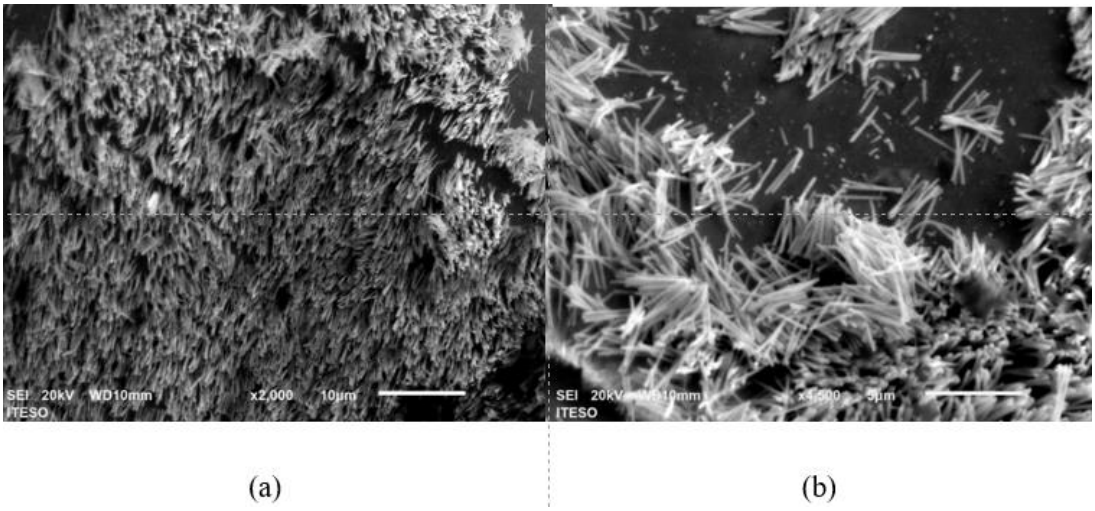

Fig. 4.4. Micrographs of the optimal length of the sensor. (a) Top view at 2000 X and (b) a view with detach nanowires from Ag film to distinguish the length of Ni NWs.

Also, the H_2O_2 concentration detection of the optimal sensor was compared with a nanostructured sensor fabricated in a previous study [López-Cárdenas-2ba], [López-Cárdenas-23b], [López-Cárdenas-21e], and with two non-optimal sensors as a benchmark (0 μm (Ni planar)) and 0.68 μm mean length nanostructured sensor used previously as an axial point; their CV and response sensitivity can be seen in Fig. 4.5.

The surroundings of the reduction peak in the CV curve were analyzed for the different H_2O_2 concentrations of 0, 0.5, 1, 1.5, 2.54, 3.25, 3.5 and 6.5 mM (inset of Fig. 4.3 (a), Fig. 4.5 (a), and Fig. 4.5 (c)). Linear regression was used to interpolate the sensor response in the range of -0.25 V to 0.25 V with a step size of 0.025 V [López-Cárdenas-21d], [Efron-16], at every *i*-th potential V. Moreover, the slope of the simple linear regression was obtained, relating the sensor response at V [*i*] to all the concentrations used. The slope of the linear regression was interpreted as the sensitivity of the sensor in units of mA/ (mM cm^2).

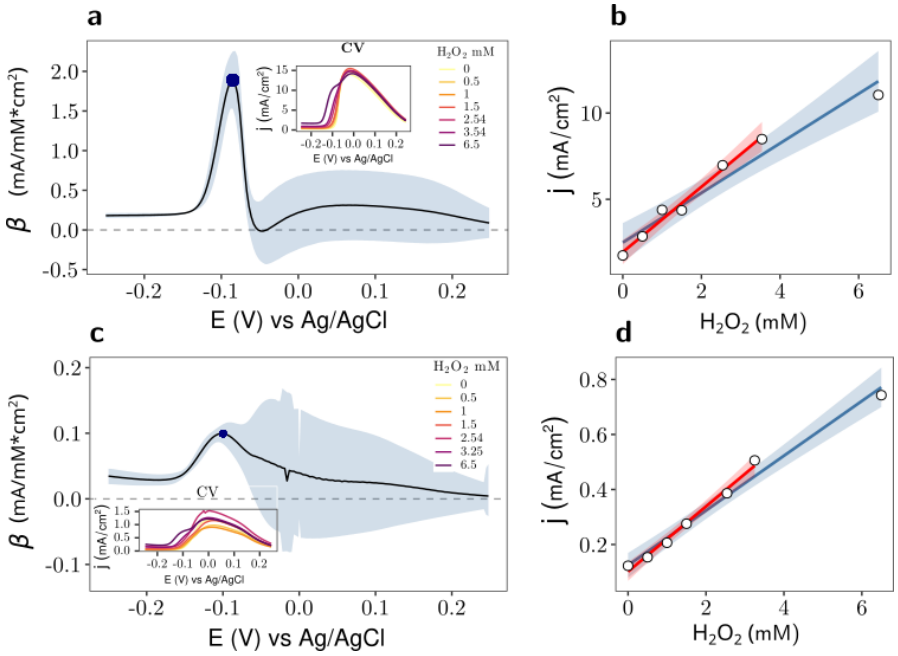

Fig. 4.5. Analysis of a non-optimum sensor that uses a 0.68 µm NW length. (a) sensitivity as a function of applied potential; the dot shows the potential at which sensitivity is maximized, (b) sensor response at the optimal potential for the different concentrations. The same goes for (c) and (d), but for the planar sensor. In both cases, the departure from linearity is smaller for the optimal sensor, as confirmed in Fig. 4.3.

Finally, our fabricated optimal NW sensor had a length of 2.62 µm with a 95% CI [2.48, 2.76] µm and showed a H_2O_2 sensitivity of 3.55 mA/(mM cm^2) with a limit of detection (LOD) of 0.78 mM H_2O_2 and a limit of quantification (LOQ) of 2.6 mMH_2O_2, significantly improved versus a planar sensor (Ni planar with a length of 0 µm) with a sensitivity of 0.1 mA/(mM cm^2), a LOD of 0.95 mM H_2O_2 and LOQ of 3.17 mM H_2O_2 and versus other fabricated as non-optimal Ni NW sensor (with a length of 0.68 µm) with a H_2O_2 sensitive of 1.55 mA/(mM cm^2), LOD of 0.81 mM H_2O_2 and LOQ of 2.71 mMH_2O_2.

Table 4.3 shows the values for comparation of the sensitivities, LOD and LOQ of Ni planar (0 µm of length) and two Ni NW sensors non-optimal 0.68 µm and the optimal with length 2.62 µm in contrast with others two sensors developed [López-Cárdenas-21b].

TABLE 4.3. COMPARISON BETWEEN SENSORS WITH DIFFERENT LENGTHS.

Material	Study	Length [μm]	Sensitivity H_2O_2 [mA/(mM*cm^2)]	LOD [mM]	LOQ [mM]
Ni	(López-Cárdenas et al., 2021)	0	0.0003	9.3	31
Ni	This study[a]	0	0.1	0.95	3.17
Ni	This study[b]	0.68	1.55	0.81	2.71
Ni	(López-Cárdenas et al., 2021)	1.2	3.02	1.53	5.1
Ni	This study[c]	2.62	3.55	0.78	2.6

[a]Ni Planar sensor, [b]Ni NW non-optimal sensor, and [c]Ni NW our optimal sensor

Our optimized sensor achieves a 50% reduction in the limit of detection (LOD) and an 18% increase in sensitivity compared with the previously investigated nanostructured sensor. Moreover, the optimized sensor is at least 35 times more sensitive for H_2O_2 detection than sensors with planar geometries, which are standard in commercial applications [López-Cárdenas-22e], [López-Cárdenas-23b].

4.3 Discussion

Were developed, manufactured and sensed the hydrogen peroxide response of two Ni sensors, one Ni planar sensor and a second nanostructured Ni NW sensor with 1.2 μm length of nanowires The data generated by these sensors from previous equipment were given to us to evaluate their behavior, allowing us to start a survey, as well as the study and analysis of data, which allowed us to report it at an international Congress, publishing it in July 2021 [López-Cárdenas 21b] in a first conference article and a second conference in November [lópez-Cardenas-

21e]. The analysis of the data was our task which allowed us to obtain and understand relevant behaviors that gave us the guideline for the development of DoE and to develop new sensors and compare their sensitivity with those previously studied. The results are shown in Table 4.3.

The response of a Ni planar (0 µm length) sensor was also measured over the same H_2O_2 concentration range from 0 mM to 3.25 mM, comparing with the optimal sensor also improved considerably with respect to this sensor, which had an LOD of 0.95 mM H_2O_2 with a sensitivity of 0.1 mA/(mM cm^2). Previously [López-Cárdenas-21b], [López-Cárdenas-21e], [López-Cárdenas-23b], an LOD of 9.3 mM H_2O_2 and a sensitivity of 0.0003 mA/(mM cm^2) for a Ni planar sensor were reported. Table 4.3 also shows a comparison with a sensor with the length of 0.68 µm at the axial point. Again, the optimal sensor performed better in all metrics. Fig. 4.6 compares the CV results of different Ni NW lengths, including the planar (line a) and optimal length (line e), and an increase in current density is observed for the 2.62 µm sensor, corresponding to our optimal value that demonstrates the non-linearity in the catalytic response [López-Cárdenas-22e], [López-Cárdenas-23a].

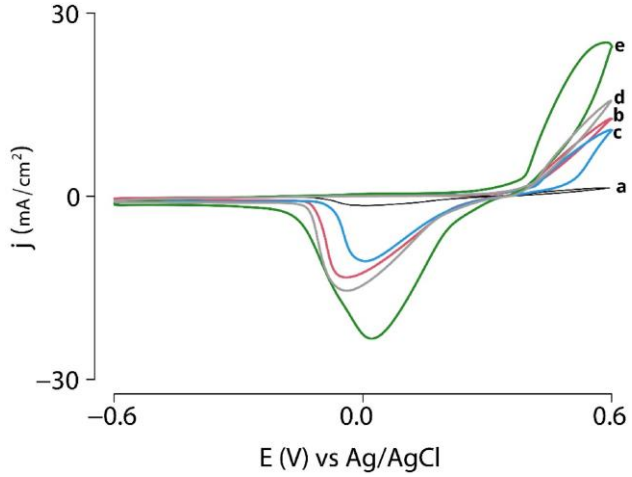

Fig. 4.6. CVs of NWs sensor in 2.54 mM H_2O_2 and PB 0.05 M pH=7 aqueous solution at a scan rate of 100 mV/s. Planar electrode in (a) and lengths of 0.68 µm in (b), 2.15 µm in (c), 3.62 µm in (d) and 2.62 µm in (e).

These results demonstrate that RSM can improve sensors based on self-supported Ni NW

arrays. The function relating the sensor response to the NW length is nonmonotonic, which could be related to the spatial disposition and formation of NWs with larger lengths, as shown in Fig. 4.7. As the size of NWs increases, they become more irregular and bent, which partially cancels the increase in response owing to the increased contact surface of the cylindrical NWs.

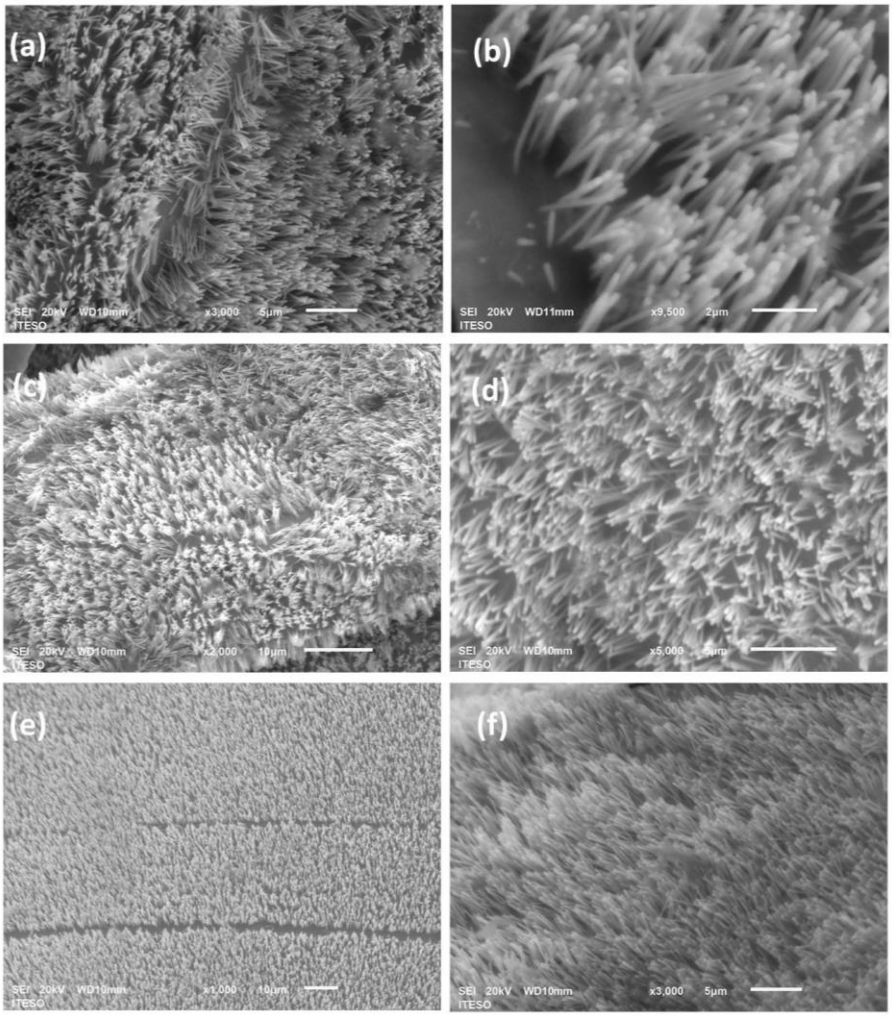

Fig. 4.7. Micrograph of self-supported Ni nanowires after removal PCTE membrane at different time depositions. (a) and (b) 3.5 minutes, (c) and (d) 4 minutes; and (e) and (f) 4.5 minutes.

General Conclusions

The development of highly sensitive sensors is a burgeoning area of research owing to the widespread potential applications of these sensors in the food industry [Buledi-22], [López-Cárdenas-21b], medical diagnostics [Wang-17], [Cheraghi-21], [López-Cárdenas-21b], [López-Cárdenas-19], [Zamfir-16], [Gupta-17], [Hwang-18], [Oliver-09], [Park-06], and environmental applications [Buledi-22], [Zhang-23], [Karimi-Maleh-23], [Meng-11]. Hence, developing a practical method to improve the design-build-test cycle of nanostructures with sensing capabilities is highly relevant and is not trivial. Although simulation studies can provide valuable information, they can be computationally restrictive as the simulations become more fine-grained, which is necessary to simulate realistic nanostructures [Goyal-20]. RSM is an efficient, theoretically agnostic (it uses generic first order and second-order functions to approximate the response), and low-cost approach to designing and evaluating nanostructured sensors. It can be easily implemented in almost all major statistical software, as it only requires estimation methods such as the ordinary least squares method [Myers-16]. With appropriate domain knowledge that can be used to select the initial testing conditions [Cheraghi-21], RSM can rapidly approximate the optimal response as a function of the design variables, as shown in this study.

This thesis was mainly focused on the study of the detection of H_2O_2 aided by RSM to optimize the design of nanostructures with sensing capabilities. One design variable of the sensors was evaluated, namely, the NW length, while varying the measurement conditions, such as the applied potential and H_2O_2 concentration, using voltametric methods. This optimal design was at least 35 times more sensitive than the planar electrode for detecting H_2O_2, which is the standard for commercial applications [López-Cárdenas-23b]. Coupled with immobilized glucose oxidase enzymes, this sensor can be used to significantly improve the detection of glucose in samples known to have low concentrations, such as tears or saliva [Liu-15], [Grupta-17], [Sánchez-Hernández-23], which are two non-invasive samples that can be used for continuous glucose monitoring in patients with diabetes mellitus.

Applied in experimental works of an electrochemical nature in nanotechnology, an RSM methodology widely used in the industry to optimize and make redesigns, reducing the number of experiments, costs, and time.

Apply data science to the large volume of information generated or actual data obtained in the experimental field (CV, SEM) using non-parametric statistics with resampling techniques, managing to determine variability measures with intervals and 95% confidence levels.

Bootstrapping a resampling method, using no parametric statistics, was employed for obtaining confidence intervals in LOD and LOQ where it is not frequent to know their variability.

Other essential design variables, such as the porous density, synthesis materials (e.g., gold), and geometrical arrangements (e.g., hexagonal versus random pore grids), require further investigation. Further investigation is also required for substances other than H_2O_2, which require different design variable levels and testing conditions.

As nanotechnology is a newer field of work and reviewing its state of the art, it was observed that, in many articles consulted, they only share results obtained for a specific nanostructure and that they manage to measure something, but their results do not present optimal results and formal validation, that is, they do not use support from mathematical tools or statistical methods.

The RSM methodology widely used in the industry to optimize and carry out redesigns, proved to be a very useful tool to apply in experimental work of an electrochemical nature, reducing the number of experiments, costs, and work times.

Applying data science to the large volume of information generated in experimental electrochemical processes (CV, SEM) contributes significantly to the study, generation, and analysis of results, using statistical techniques.

Using Bootstrap, a non-parametric statistical tool with resampling techniques, managing to determine variability measures with 95% confidence intervals and levels.

With this resampling technique, it allowed us to obtain confidence intervals in the limit of Determination (LOD) and limit of quantification (LOQ) where it is not common to know their variability.

Conclusiones generales

El desarrollo de sensores altamente sensibles es un área de investigación floreciente debido a las amplias aplicaciones potenciales de estos sensores en la industria alimentaria [Buledi-22], [López-Cárdenas-21b], diagnósticos médicos [Wang-17], [Cheraghi-21], [López-Cárdenas-21b], [López-Cárdenas-19], [Zamfir-16], [Gupta-17], [Hwang-18], [Oliver-09], [Park-06], y aplicaciones medioambientales [Buledi-22], [Zhang-23], [Karimi-Maleh-23], [Meng-11]. Por lo tanto, desarrollar un método práctico para mejorar el ciclo de diseño, construcción y prueba de nanoestructuras con capacidades de detección es muy relevante y no trivial. Aunque los estudios de simulación pueden proporcionar información valiosa, pueden ser computacionalmente restrictivos a medida que las simulaciones se vuelven más detalladas, lo cual es necesario para simular nanoestructuras realistas [Goyal-20]. RSM es un enfoque eficiente, teóricamente agnóstico (utiliza funciones genéricas de primer y segundo orden para aproximar la respuesta) y de bajo costo para diseñar y evaluar sensores nanoestructurados. Se puede implementar fácilmente en casi todas las herramientas de software estadísticas, ya que solo requiere métodos de estimación como el método de mínimos cuadrados ordinarios [Myers-16]. Con el conocimiento de dominio adecuado que se puede utilizar para seleccionar las condiciones de prueba iniciales [Cheraghi-21], RSM puede aproximarse rápidamente a la respuesta óptima en función de las variables de diseño, como se muestra en este estudio.

Esta tesis se enfocó principalmente al estudio de la detección de H_2O_2 auxiliada por técnicas de RSM para optimizar el diseño de nanoestructuras con capacidad de detección. Se evaluó una variable de diseño de los sensores, a saber, la longitud NW, variando las condiciones de medición, como el potencial aplicado y la concentración de H_2O_2 mediante métodos voltamperométricos. El diseño óptimo obtenido fue al menos 35 veces más sensible que el electrodo plano para detectar H_2O_2, que es el estándar para aplicaciones comerciales [López-Cárdenas-23b]. Junto con las enzimas glucosa oxidasa inmovilizadas, este sensor se puede usar para mejorar significativamente la detección de glucosa en muestras que se sabe que tienen bajas concentraciones, como lágrimas o saliva [Liu-15], [Grupta-17], [Sánchez-Hernández-23], que son dos muestras no invasivas que se pueden usar para monitoreo continuo de glucosa en pacientes con diabetes mellitus.

Otras variables de diseño esenciales, como la densidad de poros, los materiales de síntesis (p. ej., oro) y las disposiciones geométricas (p. ej., cuadrículas de poros hexagonales versus aleatorias), requieren una mayor investigación. También se requiere investigación adicional para sustancias distintas del H_2O_2, que requieren diferentes niveles de variables de diseño y condiciones de prueba.

Al ser la nanotecnología un campo de trabajo más nuevo y revisando su estado del arte, se observó que, en un número grande de los artículos consultados, solo comparten resultados obtenidos para una nanoestructura en específico y que logran medir algo, pero sus resultados no presentan resultados óptimos y una validación formal, es decir, no utilizan apoyos de herramientas matemáticas o métodos estadísticos.

La metodología RSM ampliamente utilizada en la industria para optimizar y realizar rediseños, demostró ser una herramienta muy útil para aplicarla en trabajos experimentales de naturaleza electroquímica, reduciendo el número de experimentos, costos y tiempos de trabajo.

Aplicar la ciencia de datos al gran volumen de información generada en procesos electroquímicos experimentales (CV, SEM) contribuyen de manera significativa al estudio, generación y análisis de resultados, utilizando técnicas estadísticas.

Utilizamos Bootstrapp, una herramienta estadística no paramétrica con técnicas de remuestreo, logrando determinar medidas de variabilidad con intervalos y niveles de confianza del 95%.

Con esta técnica de remuestreo, nos permitió obtener intervalos de confianza en el límite de Determinación (LOD) y límite de cuantificación (LOQ) donde no es frecuente conocer su variabilidad.

Appendix

A. LIST OF INTERNAL RESEARCH REPORTS

P. G. López-Cárdenas, J. D. Sanchez-Torres, and E. Araujo, “Propose a model to optimize biosensors nanostructured with inverse processes,” Internal Report *PhDEngScITESO-19-36-R*, ITESO, Tlaquepaque, Mexico, Dec. 2019.

P. G. López-Cárdenas, J. D. Sánchez-Torres, and E. Araujo, “Study and data analysis on the measurement of glucose on modified commercial sensors,” Internal Report *PhDEngScITESO-21-10-R*, ITESO, Tlaquepaque, Mexico, Oct. 2021.

P. G. López-Cárdenas, J. D. Sánchez-Torres, and E. Araujo, “Statistical evaluation to improve the sensitivity of hydrogen peroxide detection with nano-structured sensors,” Internal Report *PhDEngScITESO-21-13-R*, Tlaquepaque, Mexico, Oct. 2021.

P. G. López-Cárdenas, J. D. Sánchez-Torres, and E. Araujo, “A resampling approach for the data-based optimization of nanosensors,” Internal Report *PhDEngScITESO-21-28-R*, ITESO, Tlaquepaque, Mexico, Jul. 2021.

P. G. López-Cárdenas, J. D. Sánchez-Torres, and E. Araujo, “Electrochemical synthesis of self-supported nanowire arrays using templates,” Internal Report *PhDEngScITESO-22-10-R*, ITESO, Tlaquepaque, Mexico, Aug. 2022.

P. G. López-Cárdenas, J. D. Sánchez-Torres, and E. Araujo, “Electrochemical characterization of self-supported nanowire arrays by cyclic voltammetry,” Internal Report *PhDEngScITESO-22-14-R*, ITESO, Tlaquepaque, Mexico, Oct. 2022.

P. G. López-Cárdenas, J. D. Sánchez-Torres, and E. Araujo, “Enhancing hydrogen peroxide sensitivity of self-supported nanosensor arrays by the design of experiments,” Internal Report *PhDEngScITESO-22-15-R*, ITESO, Tlaquepaque, Mexico, Oct. 2022.

P. G. López-Cárdenas, J. D. Sánchez-Torres, and E. Araujo, “Optimization of hydrogen peroxide sensitivity of self-supported nanosensor arrays by the response surface methodology,” Internal Report *PhDEngScITESO-22-16-R*, ITESO, Tlaquepaque, Mexico, Oct. 2022.

P. G. López-Cárdenas, J. D. Sánchez-Torres, and E. Araujo, “Validation of optimized nanosensor for H_2O_2 detection by the response surface methodology,” Internal Report *PhDEngScITESO-22-17-R*, ITESO, Tlaquepaque, Mexico, Nov. 2022.

B. LIST OF PUBLICATIONS

P. G. López-Cárdenas, E. Alcalá, J. D. Sánchez-Torres and E. Araujo, "Improving self-supported nanowire arrays using response surface methodology for the synthesis of a H_2O_2 nanostructured sensor," *Materials Chemistry and Physics*, vol. 303, pp. 127729, Jul. 2023. https://doi.org/10.1016/j.matchemphys.2023.127729

P. G. López-Cárdenas, E. Alcalá, J. D. Sánchez-Torres, and E. Araujo, "A resampling approach for the data-based optimization of nanostructured sensors," *18th International Conference on Electrical Engineering, Computing Science and Automatic Control (CCE2021),* Mexico City, Mexico, Nov. 2021, pp 1-4. https://ieeexplore.ieee.org/abstract/document/9633114 doi: 10.1109/CCE53527.2021.9633114.

P. G. López-Cárdenas, E. Alcalá, J. D. Sánchez-Torres, and E. Araujo, "Improving self-supported nanowire arrays by response surface methodology," *XIV International Conference on Surfaces, Materials and Vacuum 2021*. Oct. 2021 Poster. Online. https://rei.iteso.mx/handle/11117/7971

P. G. López-Cárdenas, E. Alcalá, J. D. Sánchez-Torres, and E. Araujo, "Enhancing the sensitivity of a class of sensors: a data-based engineering approach," *IEEE 21st International Conference on Nanotechnology (NANO2021)*, Montreal, Canada, Jul. 2021, pp 221–224. https://ieeexplore.ieee.org/document/9514352 doi: 10.1109/NANO51122.2021.9514352.

F. Sánchez-Hernández, E. Márquez-Guerrero, E. Araujo, C. R. Aguilera-Galicia, J. L. Chávez-Hurtado, P. G. López-Cárdenas, and J. Ramírez-Angulo, "Development of a biosensor for the detection of glucose levels in saliva based on the oxidation and detection of hydrogen peroxide," *2023 IEEE Latin American Electron Devices Conference (LAEDC)*, Puebla, Mexico, 2023. Presented Conference and Poster. July 3-5, 2023

E. Alcalá, P. G. López-Cárdenas, J. D. Sánchez-Torres, and E. Araujo, "Statistical tools for the improvement and optimization of electrochemical sensors," *XIV International Conference on Surfaces, Materials and Vacuum 2021*. Oct. 2021 Poster. Online. https://rei.iteso.mx/handle/11117/7970

Bibliography

[Abràmoff-04] M. D. Abràmoff, P. J. Magalhães, and S. J. Ram, “Image processing with ImageJ,” *Biophotonics Int*. vol. 11, no. 7, pp. 36–42, 2004.

[Alcalá-21] E. Alcalá, P. G. López-Cárdenas, J. D. Sánchez-Torres, and E. Araujo, “Statistical tools for the improvement and optimization of electrochemical sensors,” in *XIV International Conference on Surfaces, Materials and Vacuum 2021. Oct. 2021* Poster. Online. https://rei.iteso.mx/handle/11117/7970

[Araujo-15] E. Araujo, A. Encinas, Y. Velázquez-Galván, J. M. Martínez-Huerta, G. Hamoir, E. Ferain, and L. Piraux, “Artificially modified magnetic anisotropy in interconnected nanowire networks,” *Nanoscale*, vol. 7, no. 4, pp. 1485–1490, Jan. 2015.

[Armbruster-08] D. A. Armbruster and T. Pry, “Limit of blank, limit of detection and limit of quantitation,” *The clinical biochemist reviews*, vol. 29, no. Suppl 1, p. S49, Aug. 2008.

[Bauer-22] J. A. Bauer, M. Zámocká, J. Majtán, and V. Bauerová-Hlinkoá, “Glucose oxidase, an enzyme “Ferrari”: its structure, function, production and properties in the light of various industrial and biotechnological applications,” *Biomolecules*, vol. 12, no. 3, pp. 472, Feb. 2022. https://doi.org/10.3390/biom12030472

[Box-87] G. E. P. Box and N. R. Draper, *Empirical model-building and response surfaces*. John Wiley & Sons: New Jersey, USA. 1987.

[Box-92] G. E. P. Box and K. B. Wilson, *On the experimental attainment of optimum conditions*. Breakthroughs in statistics. Springer, 1992, 270–310.

[Buledi-22] J. A. Buledi, N. Mahar, A. Mallah, A. R. Solangi, I. M. Palabiyik, N. Qambrani, F. Karimi, Y. Vasseghian, and H. Karimi-Maleh, “Electrochemical quantification of mancozeb through tungsten oxide/reduced graphene oxide nanocomposite: A potential method for environmental remediation*,” Food and Chemical Toxicology*, vol. 161, pp. 112843, Jan. 2022. https://doi.org/10.1016/j.fct.2022.112843

[Cai-18] X. Cai, E. E. L. Tanner, Ch. Lin, K. Ngamchuea, J. S. Foord, and R. G. Compton, “The mechanism of electrochemical reduction of hydrogen peroxide on silver nanoparticles,” *Physical Chemistry Chemical Physics*, vol. 20, no. 3, pp. 1608-1614, Jan. 2018.

[Calin-Jageman-19] R. J. Calin-Jageman and G. Cumming, “The new statistics for better science: Ask how much, how uncertain, and what else is known,” *The American Statistician*, vol. 73, no. sup1, pp. 271–280, Mar. 2019.

[Chan-19] K. S. Chan, S. J. Greaves, and S. Rahardja. “Techniques for addressing saddle points in the response surface methodology (RSM)”. *IEEE Access* (2019), 85613–85621. doi: 10.1109/ACCESS. 2019.2922975.

[Chen-13] S. Chen, R. Yuan, Y. Chai, and F. Hu, “Electrochemical sensing of hydrogen peroxide using metal nanoparticles: a review,” *Microchimica Acta*, vol 180, pp. 15-32, Jan. 2013.

[Chen-12] W. Chen, S. Cai, Q. Q. Ren, W. Wen, and Y. D. Zhao, "Recent advances in electrochemical sensing for hydrogen peroxide: a review," *Analyst*, vol. 137, no. 1, pp. 49–58, Nov. 2012.

[Cheraghi-21] S. Cheraghi, M. A. Taher, H. Karimi-Maleh, F. Karimi, M. Shabani-Nooshabadi, M. Alizadeh, A. Al-Othman, N. Erk, P. K. Yegya Raman, and C. Karaman, "Novel enzymatic graphene oxide based biosensor for the detection of glutathione in biological body fluids," *Chemosphere*, vol. 287, pp. 132187, Sep. 2021. https://doi.org/10.1016/j.chemosphere.2021.132187

[Chihara-18] L. M. Chihara and T. C. Hesterberg, *Mathematical statistics with resampling and R*. John Wiley & Sons, 2018.

[Cleveland-79] W. S. Cleveland, "Robust locally weighted regression and smoothing scatterplots," *J. Am. Stat. Assoc*. vol. 74, no. 368, pp.829–836, Dec. 1979.

[Croarkin-12] C. Croarkin, and P. Tobias, *e-Handbook of Statistical Methods* [Online]. NIST/ SEMATECH: 2012; pp Ch. 5 https://www.itl.nist.gov/div898/handbook/ (accessed Oct 26, 2021).

[Cui-08] X. Cui, Z. Li, Y. Yang, W. Zhang, and Q. Wang, "Low- potential sensitive hydrogen peroxide detection based on nanotubular TiO2 and platinum composite electrode," *Electroanalysis*, vol. 20 no. 9, pp. 970-975, Apr. 2008.

[Cumming-05] G. Cumming and S. Finch, "Inference by eye: confidence intervals and how to read pictures of data." *American psychologist*, vol. 60, no. 2, pp. 170, Mar. 2005.

[Cumming-13] G. Cumming, "Understanding the new statistics: Effect sizes, confidence intervals, and meta-analysis," *Routledge*, Jan. 2013.

[Dickinson-14] E. J. F. Dickinson, H. Ekström, and E. Fontes, "COMSOL Multiphysics®: Finite element software for electrochemical analysis. A mini-review," *Electrochem commun*. vol. 40, pp. 71-74, Mar. 2014.

[Efron-16] B. Efron and T. Hastie, *Computer age statistical inference*. Cambridge University Press, 2016, vol. 5.

[Efron-86] B. Efron, and R. Tibshirani, "Bootstrap methods for standard errors, confidence intervals, and other measures of statistical accuracy," *Statistical Science*. vol. 1, no. 1, pp. 54-77, Feb. 1986.

[Geng-13] Z. Geng, F. Yang, M. Li, and N. Wu, "A bootstrapping-based statistical procedure for multivariate calibration of sensor arrays," *Sensors and Actuators B: Chemical*, vol. 188, pp. 440–453, Nov. 2013.

[Ghanei-Motlagh-19] M. Ghanei-Motlagh, M. A. Taher, M. Fayazi, M. Baghayeri, and A. R. Hosseinifar, "Non-enzymatic amperometric sensing of hydrogen peroxide based on vanadium pentoxide nanostructures," *J. Electrochem. Soc.*, vol. 166, pp. B367-B373. Mar. 2019.

[Good-13] P. I. Good, *Introduction to statistics through resampling methods and R*. John Wiley & Sons, 2013.

[Goyal-20] H. Goyal, and D. G. Vlachos, "Multiscale modeling of microwave-heated multiphase systems," *Chem. Eng. J*., vol. 397, pp. 125262, Oct. 2020.

[Guideline-05] I. H. T. Guideline et al., "Validation of analytical procedures: text and methodology," *Q2 (R1)*, vol. 1, no. 20, p. 05, Jun. 2005

[Gupta-17] S. Gupta, S. Tyler, A. Banaszak, and J. Boeckl, "Graphene quantum dots electrochemistry and sensitive electrocatalytic glucose sensor development," *Nanomaterials*, vol. 7, no. 301, pp. 1-20, Oct. 2017.

[Gutiérrez Pulido-12] H. Gutiérrez Pulido, R. De la Vara Salazar, *Análisis y diseño de experimentos.* McGraw Hill, 2012.

[Hayfield-08] T. Hayfield and J. S. Racine, "Nonparametric econometrics: The np package," Journal of Statistical Software, vol. 27, no. 5, Jul. 2008. [Online]. Available: http://www.jstatsoft.org/v27/i05/

[Hocking-03a] R. R. Hocking, *Introduction to linear models, in methods and applications of linear models: regression and the analysis of variance, part I: Regression models. 1. Introduction to linear models*. [Wiley Series in Probability and Statistics], 2nd ed., J. Wiley, Ed. Wiley, 2003, pp. 1–21.

[Hocking-03b] R. R. Hocking, *Introduction to analysis of variance models, in methods and applications of linear models: Regression and the analysis of variance, part II Analysis of variance. 9. Introduction to analysis of variance models*. [Wiley Series in Probability and Statistics], J. Wiley, Ed. Wiley, 2003, pp. 294–308.

[Hua-11] M. Y. Hua, H. C. Chen, C. K. Chuang, R. Y. Tsai, J. L. Jeng, H. W. Yang, and Y. T. Chern, "The intrinsic redox reactions of polyamic acid derivatives and their application in hydrogen peroxide sensor," *Biomaterials*, vol. 32, no. 21, pp. 4885–4895, Jul. 2011.

[Hwang-18] D. W. Hwang, S. Lee, M. Seo, and T. D. Chung, "Recent advances in electrochemical non-enzymatic glucose sensors – A review," *Analytica Chimica Acta*, vol. 1033. Elsevier B.V., pp. 1–34, Nov. 2018.

[James-13] G. James, D. Witten, T. Hastie, and R. Tibshirani, *An introduction to statistical learning*. Springer Texts in Satistics, 2013, vol. 112.

[Jia-09] W. Jia, M. Guo, Z. Zheng, T. Yu, E. G. Rodriguez, Y. Wang, and Y. Lei, "Electrocatalytic oxidation and reduction of H2O2 on vertically aligned Co3O4 nanowalls electrode Toward H_2O_2 detection," *Journal of Electroanalytical Chemistry*, vol. 625, no. 1, pp. 27–32, Sep. 2009.

[Karimi-Maleh-23] H. Karimi-Maleh, R. Darabi, F. Karimi, C. Karaman, S. A. Shahidi, N. Zare, M. Baghayeri, L. Fu, S. Rostamnia, J. Rouhi, and S. Rajendran, "State-of-art advances on removal, degradation and electrochemical monitoring of 4-aminophenol pollutants in real samples: A review," *Environmental Research*, vol. 222, pp. 115338, 2023. https://doi.org/10.1016/j.envres.2023.115338

[Keithley-11] I. Keithley*, "Series 2400 SourceMeter® User's Manual," Keithley*. Keithley Instruments, Inc. Corporate, Cleveland, Ohio, pp. 1–496, Sep. 2011. [Online]

[Kyprioti-20] A. P. Kyprioti, J. Zhang, and A. A. Taflanidis, "Adaptive design of experiments for global kriging metamodeling through cross-validation information," *Structural and Multidisciplinary Optimization*, vol. 62, no. 3, pp. 1135–1157, Mar. 2020.

[Lawson-14] J. Lawson, *Design and Analysis of Experiments with R*; CRC press: Florida, 2014.

[Length-20] R. V. Lenth, "Response-Surface Methods in R, Using rsm," *J. Stat. Softw*. 2009, 32(7), 1–17. //Sep. 2020.

[Liu-15] C. Liu, Y. Sheng, Y. Sun, J. Feng, S. Wang, J. Zhang, and X. Jiacui, "A glucose oxidase-coupled DNAzyme sensor for glucose detection in tears and saliva," *Biosens. Bioelectron*, vol. 70, pp. 455-461, Mar. 2015.

[López-Cárdenas-19] P. G. López-Cárdenas, E. Araujo, and J. D. Sánchez-Torres, "Propose a model to optimize biosensors nanostructured with inverse processes," Internal Report *PhDEngScITESO-19-36-R*, ITESO, Tlaquepaque, Mexico, Dec. 2019.

[López-Cárdenas-21a] P. G. López-Cárdenas, E. A. Araujo-Palomo and J. D. Sánchez-Torres, "A resampling approach for the data-based optimization of nanosensors," Internal Report *PhDEngScITESO-21-28-R*, ITESO, Tlaquepaque, Mexico, Jul. 2021.

[López-Cárdenas-21b] P. G. López-Cárdenas, E. Alcalá, J. D. Sánchez-Torres and E. Araujo, "Enhancing the sensitivity of a class of sensors: a data-based engineering approach," in *IEEE 21st International Conference on Nanotechnology (NANO2021*), Montreal, Canada, Jul. 2021, pp 221–224. doi:10.1109/NANO51122.2021.9514352. https://ieeexplore.ieee.org/document/9514352

[López-Cárdenas-21c] P. G. López-Cárdenas, E. E. Araujo-Palomo, and J. D. Sánchez-Torres, "Study and data analysis on the measurement of glucose on modified commercial sensors," Internal Report *PhDEngScITESO-21-10-R*, ITESO, Tlaquepaque, Mexico, Oct. 2021.

[López-Cárdenas-21d] P. G. López-Cárdenas, E. E. Araujo-Palomo, and J. D. Sánchez-Torres, "Statistical evaluation to improve the sensitivity of hydrogen peroxide detection with nano-structured sensors," Internal Report *PhDEngScITESO-21-13-R*, Tlaquepaque, Mexico, Oct. 2021.

[López-Cárdenas-21e] P. G. López-Cárdenas, E. Alcalá, J. D. Sánchez-Torres and E. Araujo, "Improving self-supported nanowire arrays by response surface methodology," in *XIV International Conference on Surfaces, Materials and Vacuum 2021*. Zacatecas, Mexico, Oct. 2021 Poster. Online. https://rei.iteso.mx/handle/11117/7971.

[López-Cárdenas-21f] P. G. López-Cárdenas, E. Alcalá, J. D. Sánchez-Torres and E. Araujo, "A resampling approach for the data-based Optimization of nanosensors," in *18th International Conference on Electrical Engineering, Computing Science and Automatic Control (CCE-2021)*, Mexico City, Mexico, 2021, pp. 1-4, doi: 10.1109/CCE53527.2021.9633114. https://ieeexplore.ieee.org/abstract/document/9633114

[López-Cárdenas-22a] P. G. López-Cárdenas, E. A. Araujo-Palomo and J. D. Sánchez-Torres, "Electrochemical synthesis of self-supported nanowire arrays using templates," Internal Report *PhDEngScITESO-22-10-R*, ITESO, Tlaquepaque, Mexico, Aug. 2022.

[López-Cárdenas-22b] P. G. López-Cárdenas, E. A. Araujo-Palomo and J. D. Sánchez-Torres, "Electrochemical characterization of self-supported nanowire arrays by cyclic voltammetry," Internal Report *PhDEngScITESO-22-14-R*, ITESO, Tlaquepaque, Mexico, Oct. 2022.

[López-Cárdenas-22c] P. G. López-Cárdenas, E. A. Araujo-Palomo and J. D. Sánchez-Torres, "Enhancing hydrogen peroxide sensitivity of self-supported nanosensor arrays by the design of experiments," Internal Report *PhDEngScITESO-22-15-R*, ITESO, Tlaquepaque, Mexico, Oct. 2022.

[López-Cárdenas-22d] P. G. López-Cárdenas, E. A. Araujo-Palomo and J. D. Sánchez-Torres, "Optimization of hydrogen peroxide sensitivity of self-supported nanosensor arrays by the response surface

methodology," Internal Report *PhDEngScITESO-22-16-R*, ITESO, Tlaquepaque, Mexico, Oct. 2022.

[López-Cárdenas-22e] P. G. López-Cárdenas, E. A. Araujo-Palomo and J. D. Sánchez-Torres, "Validation of optimized nanosensor for hydrogen peroxide detection by the response surface methodology," Internal Report *PhDEngScITESO-22-17-R*, ITESO, Tlaquepaque, Mexico, Nov. 2022.

[López-Cárdenas-23a] P. G. López-Cárdenas, E. Alcalá, J. D. Sánchez-Torres and E. Araujo, "Improving self-supported nanowires array using response surface methodology for the synthesis of an H_2O_2 nanosensor." [Online] Available at SSRN: https://ssrn.com/abstract=4362700 or http://dx.doi.org/10.2139/ssrn.4362700 ELSEVIER

[López-Cárdenas-23b] P. G. López-Cárdenas, E. Alcalá, J. D. Sánchez-Torres and E. Araujo, "Improving self-supported nanowire arrays using response surface methodology for the synthesis of a H_2O_2 nanostructured sensor," *Materials Chemistry and Physics*, vol. 303, pp. 127729, Jul. 2023. https://doi.org/10.1016/j.matchemphys.2023.127729

[Meng-11] F. Meng, X. Yan, J. Liu, J. Gu, and Z. Zou, "Nano porous gold as non-enzymatic sensor for hydrogen peroxide," *Electrochimica Acta*, vol. 56, pp. 4657-4662, Mar. 2011.

[Montgomery-17] D. C. Montgomery. *Design and Analysis of Experiments*. John Wiley & Sons: New Jersey, USA. 2017.

[Musa-12] S. M. Musa. *Computational Finite Element Methods in Nanotechnology*. Taylor & Francis Group/CRC Press: Florida, USA. 2012.

[Myers-16] R. H. Myers, D. C. Montgomery, and C. M. Anderson-Cook. *Response surface methodology: process and product optimization using designed experiments.* John Wiley & Sons: New Jersey, USA. 2016.

[Nasirpouri-17] F. Nasirpouri, *Electrodeposition of Nanostructured Materials*. Springer: New York, 2017.

[Olarte-13] O. Olarte, J. Chilo, J. Pelegri-Sebastia, K. Barbé, and W. Van Moer, "Glucose detection in human sweat using an electronic nose," *in 35th Annual International Conference of the IEEE Engineering in Medicine and Biology Society (EMBC*), Sep. 2013, pp. 1462–1465.

[Oliver-09] N. S. Oliver, C. Toumazou, A. E. G. Cass, and D. G. Johnston, "Glucose sensors: A review of current and emerging technology," *Diabet. Med.*, vol. 26, no. 3, pp. 197–210, Nov. 2009.

[Park-06] S. Park, H. Boo, and T. D. Chung, "Electrochemical non-enzymatic glucose sensors," *Anal. Chim. Acta*, vol. 556, no. 1, pp. 46–57, Jan. 2006.

[Paternoster-98] R. Paternoster, R. Brame, P. Mazerolle, and A. Piquero, "Using the correct statistical test for the equality of regression coefficients," Criminology, vol. 36, no. 4, pp. 859– 866, Nov. 1998.

[Qiao-12] L. Qiao, J. Xu, A. Sane, and J. Gore, "Multiphysics modeling of carbon gasification processes in a well-stirred reactor with detailed gas-phase chemistry," *Combust. Flame*, vol. 159, no. 4, pp. 1693–1707, Apr. 2012.

[Rahman-19] M. M. Rahman, M. M. Hussain, and A. M. Asiri, "dglucose sensor based on ZnO – V2O5 NRs by an enzyme-free electrochemical approach," *RSC advances*, vol. 9, no. 54, pp. 31 670–31 682, Oct. 2019.

[Rojo-Álvarez-18] J. L. Rojo-Álvarez, M. Martínez-Ramón, J. M. Marí, and G. Camps-Valls, *Digital signal processing with Kernel methods*. Wiley Online Library, Feb. 2018.

[Sánchez-Hernández-23] F. Sánchez-Hernández, E. Márquez-Guerrero, E. Araujo, C. R. Aguilera-Galicia, J. L. Chávez-Hurtado, P. G. López-Cárdenas, and J. Ramírez-Angulo, "Development of a Biosensor for the Detection of Glucose Levels in Saliva Based on the Oxidation and Detection of Hydrogen Peroxide," in *IEEE Latin American Electron Devices Conference (LAEDC2023*), Puebla, Mexico, 2023. Presented Conference and Poster. July 3-5, 2023.

[Satish-14] L. Stahle and W. Svante, "Analysis of Variance (ANOVA)," *Chemom. Intell. Lab. Syst*., vol. 6, no. 4, pp. 259–272, Jul. 1989.

[Stahle-89] J. G. Servín-Aguilar, L. Rizo-Domínguez, and J. A. Pardiñas-Mir, "A comparison between wavelet families to compress an EEG signal," in *IEEE ANDESCON Proc.*, Arequipa, Peru, Oct. 2016, pp. 1-4.

[Thomas-17] S. Thomas, R. Thomas, A. K. Zachariah, and R. K. Mishra, *Spectroscopic Methods for Nanomaterials Characterization*, Cambridge, MA: Elsevier, May. 2017, vol. 2.

[Van-Beers-08] W. C. M. Van Beers, and J. P. C. Kleijnen, "Customized sequential designs for random simulation experiments: Kriging metamodeling and bootstrapping," *European journal of operational research*, vol. 186, no. 3, pp. 1099–1113, May. 2008.

[Viveros-Wacher-16] A. Viveros-Wacher and J. E. Rayas-Sánchez, "Eye diagram optimization based on design of experiments (DoE) to accelerate industrial testing of high speed links," in *IEEE MTT-S Latin America Microwave Conf. (LAMC-2016)*, Puerto Vallarta, Mexico, Dec. 2016, pp. 1-3.

[Wang-17] Z. Wang, X. Cao, D. Liu, S. Hao, R. Kong, G. Du, A. M. Asiri, and X. Sun, "Copper nitride nanowires array: an efficient dual-functional catalyst electrode for sensitive and selective non-enzymatic glucose and hydrogen peroxide sensing," *Chem. Eur. J*. vol. 23, no. 21, pp. 4986-4989, Apr. 2017.

[Wasserman-04] L. Wasserman, *All of statistics: a concise course in statistical inference*. Springer Science+Business Media, 2004.

[Zamfir-16] L. G. Zamfir, L. Rotariu, V. E. Marinescu, X. T. Simelane, P. G. L. Baker, E. I. Iwuoha, and C. Bala, "Non-enzymatic polyamic acid sensors for hydrogen peroxide detection", *Sensors and Actuators B: Chemical*, vol. 226, pp. 525-533, Apr. 2016.

[Zhang-23] Z. Zhang, and H. Karimi-Maleh, "In situ synthesis of label-free electrochemical aptasensor-based sandwich-like AuNPs/PPy/Ti3C2Tx for ultrasensitive detection of lead ions as hazardous pollutants in environmental fluids," *Chemosphere*, pp. 138302, 2023. https://doi.org/10.1016/j.chemosphere.2023.138302

[Zong-17] C. Zong, M. Wang, B. Li, X. Liu, W. Zhao, Q. Zhang, A. Liang, and Y. Yu, "Sensing of hydrogen peroxide and glucose in human serum via quenching fluorescence of biomolecule-stabilized Au nanoclusters assisted by the Fenton reaction," *RSC adv*. vol. 7, no. 43, pp. 26559-26565, May. 2017.

Author Index

Subject Index

S

T

V

W